

1 **Homogenized century-long surface incident solar radiation**  
2 **over Japan**

3 Qian Ma<sup>1</sup>, Kaicun Wang\*<sup>1</sup>, Yanyi He<sup>1</sup>, Liangyuan Su<sup>1</sup>, Qizhong Wu<sup>1</sup>, Han Liu<sup>1</sup>, Youren  
4 Zhang<sup>1</sup>

5  
6 <sup>1</sup>State Key Laboratory of Earth Surface Processes and Resource Ecology, College of  
7 Global Change and Earth System Science, Beijing Normal University, Beijing 100875,  
8 China

9  
10 **Submitted to *Earth System Science Data***

11  
12 **Corresponding Author:** Dr. Kaicun Wang, State Key Laboratory of Earth Surface  
13 Processes and Resource Ecology, College of Global Change and Earth System Science,  
14 Beijing Normal University, Beijing, 100875, China. Email: [kewang@bnu.edu.cn](mailto:kewang@bnu.edu.cn); Tel.:  
15 +86 (10)-58803143.

16  
17 **November 16, July 3, 2021**

域代码已更改

带格式的: 字体颜色: 自动设置

带格式的: 字体颜色: 自动设置

Abstract

20

21

22

23

24

25

26

27

28

29

30

31

32

33

34

35

36

37

38

39

40

Surface incident solar radiation ( $R_s$ ) plays an essential key role in climate change on Earth.  $R_s$  can be directly measured, and it shows substantial variability on decadal scales, i.e., global dimming and brightening, ~~on decadal scales~~.  $R_s$  can also be derived from the observed sunshine duration (SunDu) with reliable accuracy. The SunDu-derived  $R_s$  ~~has been~~ was used as a reference to detect and adjust the inhomogeneity in the observed  $R_s$ . However, both the observed  $R_s$  and SunDu-derived  $R_s$  may have inhomogeneity. In Japan, SunDu has been measured since 1890, and  $R_s$  has been measured since 1961 at ~100 stations. In this study, the observed  $R_s$  and SunDu-derived  $R_s$  were first checked for inhomogeneity independently using ~~with the a~~ statistical software RHtest. If confirmed by the metadata of these observations, the detected inhomogeneity was adjusted based on the RHtest-quantile matching method. Second, the two homogenized time series were compared to detect further possible inhomogeneity. If confirmed by the independent ground-based manual observations of cloud cover fraction, the detected inhomogeneity was adjusted based on the reference dataset. As a result, a sharp decrease of more than 20 W m<sup>-2</sup> in the observed  $R_s$  from 1961 to 1975 caused by instrument displacement was detected and adjusted. Similarly, a ~~gradual~~ decline of about 20 W m<sup>-2</sup> in SunDu-derived  $R_s$  due to steady instrument replacement from 1985 to 1990 was detected and adjusted too. After homogenizations, the two estimates of  $R_s$  agree well. The homogenized SunDu-derived  $R_s$  was found to ~~have~~ show an increased at a rate of 0.9 W m<sup>-2</sup> per decade ( $p < 0.01$ ) from 1961 to 2014~~5~~.

41 ~~based on the homogenized SunDu derived  $R_s$~~ , which was ~~enhanced~~caused by a positive  
42 aerosol-related radiative effect ( $2.2 \text{ W m}^{-2}$  per decade) and ~~diminished by~~ a negative  
43 cloud cover radiative effect ( $-1.4 \text{ W m}^{-2}$  per decade). The brightening over Japan was  
44 the strongest in spring, likely due to a significant decline in aerosol transported from  
45 Asian dust storms. The observed raw  $R_s$  data and their homogenized time series used in  
46 this study are available at <https://doi.org/10.11888/Meteoro.tpsc.271524> (Ma et al.,  
47 2021).

带格式的: 字体颜色: 自动设置

带格式的: 字体颜色: 自动设置

#### 49 **Key Points:**

- 50 ~~(1) Surface incident solar radiation ( $R_s$ ) and sunshine duration over Japan were~~  
51 ~~homogenized.~~
- 52 ~~(2) Homogenized century long  $R_s$  data over Japan were produced, and shows that  $R_s$~~   
53 ~~increased at a rate of  $\sim 1 \text{ W m}^{-2}$  per decade from 1961 to 2015.~~
- 54 ~~(3) Cloud cover modulates  $R_s$  variation at monthly and interannual time scales, while~~  
55 ~~aerosols dominate the decadal variation in  $R_s$ .~~

带格式的: 字体颜色: 自动设置

## 56 1. Introduction

57 Surface incident solar radiation ( $R_s$ ) plays a vital role in atmospheric circulation,  
58 hydrologic cycling and ecological equilibrium; therefore, its decrease and increase  
59 termed as global dimming and brightening (Wild et al., 2005; Shi et al., 2008), have  
60 received widespread interest from the public and scientific community (Allen et al.,  
61 2013; Xia, 2010; Wang et al., 2013; Tanaka et al., 2016; Ohmura, 2009; He et al., 2018).

62 In addition, the impact factors such as clouds and aerosols on the variation in  $R_s$  have  
63 been widely studied (Wild et al., 2021; Qian et al., 2006; Feng and Wang, 2021a).

64 Ground-based observations of  $R_s$  are the first recommendation for detecting global  
65 dimming and brightening. However, observational data may be inevitably ruined by  
66 artificial shifts, which may lead to the variability in  $R_s$  with large  
67 uncertainties. Instrument replacements introduced substantial inhomogeneity into the  
68 time series of observed  $R_s$  over China during the period of 1990–1993. Wang et al. (2015)

69 point out that instrument replacements and reconstruction of observational network  
70 introduced substantial inhomogeneity into the time series of observed  $R_s$  over China for  
71 1990–1993. Instrument changes from the Robitzsch pyranograph to the Kipp & Zonen  
72 CM11 pyranometer before 1980 caused no clear dimming in Italy. Manara et al. (2016)

73 also show the instrument changes from the Robitzsch pyranograph to the Kipp & Zonen  
74 CM11 pyranometer before 1980 caused no clear dimming in Italy. Until recently,  
75 Wild et al. (2021) use a well-maintained data series at a site in Germany with long time

域代码已更改

域代码已更改

域代码已更改

域代码已更改

域代码已更改

76 duration to investigate the dimming and brightening in central Europe under clear sky  
77 condition, and point out that the aerosol pollutants are likely major drivers in the  $R_s$   
78 variations. Augustine and Hodges (2021) use Surface Radiation Budget (SURFRAD)  
79 Network observations to explore the variability in  $R_s$  over the U.S. from 1996 to 2019,  
80 and find that cloud fraction can explain 62% of the variation of  $R_s$ , while aerosol optical  
81 depth (AOD) only accounts for 3%. Both studies also indicate the measurement  
82 instruments have been changed over the observational time periods, which may  
83 introduce non-climatic shifts and inhomogeneity in the raw data series.  $R_s$  can be  
84 measured by either a single pyranometer or the summation of diffuse and direct  
85 components. The measurement of  $R_s$ , which started in 1961 in Japan, has a long history  
86 (Tanaka et al., 2016), and a data record more than half a century long has been  
87 accumulated. The dataset has been widely used to study decadal variability (Wild et al.,  
88 2005; Stanhill and Cohen, 2008) and to evaluate model simulations (Allen et al., 2013;  
89 Dwyer et al., 2010).

域代码已更改

域代码已更改

域代码已更改

域代码已更改

90 The Eppley and Robitzsch pyranometers used to measure  $R_s$  over Japan were  
91 replaced by the Moll-Gorezynski thermopile pyranometers in the early 1970s (Tanaka  
92 et al., 2016). However, the possible homogeneity of the observed  $R_s$  over Japan has not  
93 been well quantified, and most existing studies directly used raw  $R_s$  data (Wild et al.,  
94 2005; Tanaka et al., 2016; Tsutsumi and Murakami, 2012; Allen et al., 2013; Wild and  
95 Schmucki, 2011; Kudo et al., 2012; Ohmura, 2009). Some studies have had to abandon  
96 data from the early years and focused on only  $R_s$  data collected after 1975 (Tsutsumi

域代码已更改

域代码已更改

域代码已更改

97 ~~and Murakami, 2012; Dwyer et al., 2010). Therefore, the observed decadal variability~~  
98 ~~in  $R_s$  over Japan is questionable, especially for the 1961–1975 time period.~~

99 Homogenizing the observed  $R_s$  has been attempted in China (Wang et al., 2015;  
100 Tang et al., 2011; Yang et al., 2018), Italy (Manara et al., 2016), Spain (Sanchez-  
101 Lorenzo et al., 2013) and Europe (Sanchez-Lorenzo et al., 2015). It is essential to find  
102 a homogeneous reference station to compare with the possible inhomogeneous station  
103 to test and adjust the inhomogeneity in the observed time series, as done for the  
104 homogenization of air temperature (Du et al., 2020; Zhou et al., 2021). However, this  
105 process is difficult for  $R_s$  because the instrument replacement of  $R_s$  generally occurs  
106 nearly simultaneously throughout a country. Therefore, the sunshine duration (SunDu)  
107 -derived  $R_s$  (Yang et al., 2006) has been used as a homogeneous reference dataset to  
108 detect and adjust the inhomogeneity of  $R_s$  in China (Wang et al., 2015).

109 The SunDu records the hours of surface direct solar radiation exceeding  $120 \text{ W m}^{-2}$   
110 and provides an alternative way to estimate  $R_s$  (Yang et al., 2006; Stanhill and Cohen,  
111 2008). ~~SunDu-derived  $R_s$  is capable of capturing the variability in  $R_s$ .~~ He et al. (2018)  
112 ~~use the SunDu-derived  $R_s$  at ~2600 stations to revisit the global dimming and~~  
113 ~~brightening over different continents, and restate the dimming over China and Europe~~  
114 ~~is consistent with the increasing trends of clouds and aerosols.~~ Feng and Wang (2021b)  
115 ~~and Feng and Wang (2021a) merge the satellite retrievals with SunDu-derived  $R_s$  to~~  
116 ~~produce a high-resolution long-term solar radiation over China, and indicate cloud~~  
117 ~~fraction could explain approximately 86%–97% of  $R_s$  variation.~~ Zeng et al. (2020)

域代码已更改

域代码已更改

域代码已更改

域代码已更改

域代码已更改

域代码已更改

域代码已更改

域代码已更改

域代码已更改

域代码已更改

域代码已更改

域代码已更改

域代码已更改

118 demonstrate that SunDu plays a dominant role in determining  $R_s$  based on a random  
119 forest model framework across China. Stanhill and Cohen (2005) indicate the high  
120 correlation between SunDu and  $R_s$  at the 26 stations in the United States. Sanchez-  
121 Lorenzo et al. (2008) show the variation in SunDu is consistent with that in  $R_s$  over  
122 western Europe for 1938-2004, and the SunDu time evolution in Spring can partly be  
123 explained by clouds and that in Winter can be related to the anthropogenic aerosol  
124 emissions. Stanhill and Cohen (2008) establish a simple linear relationship between  $R_s$   
125 and SunDu to determine the long-term variation in  $R_s$  over Japan. Manara et al. (2017)  
126 highlight that the atmospheric turbidity should be considered when using SunDu for  
127 investigating multidecadal evolution of  $R_s$ .

128 Artificial shifts in SunDu observations may come from the replacement of  
129 instruments. It has been revealed that the Jordan recorder is 10% more sensitive than  
130 the Campbell-Stokes recorder for SunDu measurements (Noguchi, 1981). The  
131 homogenization of SunDu has been carried out in Iberian Peninsula (Sanchez-Lorenzo  
132 et al., 2007), Switzerland (Sanchez-Lorenzo and Wild, 2012), and Italy (Manara et al.,  
133 2015).

134 The measurement of  $R_s$ , which started in 1961 in Japan, has a long history (Tanaka  
135 et al., 2016), and a data record more than half a century-long has been accumulated.  
136 The dataset has been widely used to study decadal variability (Wild et al., 2005; Stanhill  
137 and Cohen, 2008) and to evaluate model simulations (Allen et al., 2013; Dwyer et al.,  
138 2010). The Eppley and Robitzsch pyranometers used to measure  $R_s$  over Japan were

域代码已更改

域代码已更改

域代码已更改

域代码已更改

域代码已更改

域代码已更改

域代码已更改

域代码已更改

域代码已更改

域代码已更改

域代码已更改

139 replaced by the Moll-Gorczynski thermopile pyranometers in the early 1970s (Tanaka  
140 et al., 2016). However, the possible inhomogeneity of the observed  $R_s$  over Japan has  
141 not been well quantified, and most existing studies directly used raw  $R_s$  data (Wild et  
142 al., 2005; Tanaka et al., 2016; Tsutsumi and Murakami, 2012; Allen et al., 2013; Wild  
143 and Schmucki, 2011; Kudo et al., 2012; Ohmura, 2009). Some studies have had to  
144 abandon data from the early years and focused on only  $R_s$  data collected after 1975  
145 (Tsutsumi and Murakami, 2012; Dwyer et al., 2010). Therefore, the observed decadal  
146 variability in  $R_s$  over Japan is questionable, especially for the 1961-1975 time period.

147 In Japan, SunDu observations started in 1890, and more than a century-long data  
148 were recorded. They cannot be too precious for the climate change detection on a  
149 century scale. It is reported that the Jordan recorders used to measure SunDu were  
150 replaced by EKO rotating mirror recorders in approximately 1986 (Inoue and  
151 Matsumoto, 2003; Stanhill and Cohen, 2008). Therefore, SunDu observations over  
152 Japan themselves may ~~have suffer~~ inhomogeneity issues.

153 Non-climatic shifts in the observations may severely influence the climate  
154 assessment, therefore rigorous homogenization are required. The world Meteorological  
155 Organization (WMO) Climate Program guidelines on climate metadata and  
156 homogenization list 14 data homogenization assessment techniques developed and  
157 applied by different groups/authors (Aguilar et al., 2003). Reeves et al. (2007)  
158 compared eight representative homogenization methods and provided guidelines for  
159 which procedures work best in different situation, for example the standard normal

域代码已更改

域代码已更改

域代码已更改

域代码已更改

域代码已更改

域代码已更改



160 homogeneity (SNH) test (Alexandersson, 1986) works best if good reference series are  
161 available and two-phase regressions of Wang procedure (Wang, 2003) is optimal for  
162 good reference series unavailable condition. Based on the comparison work, RHtest  
163 method was improved by detecting multiple changepoints in the climate data no matter  
164 the reference series are available (Wang, 2008b; Wang et al., 2010; Wang et al., 2007;  
165 Wang, 2008a). This method, which first detects the changepoints in a series using  
166 penalized maximal tests and then tunes the inhomogeneous data segments to be  
167 consistent with other segments in empirical distributions, has been widely used in  
168 homogenizing climate variables~~The RHtest quantile matching (QM) method, which~~  
169 ~~first detects the changepoints in a series and then tunes the inhomogeneous data~~  
170 ~~segments to be consistent with other segments in empirical distributions, has been~~  
171 ~~widely used for homogenizing climate variables (Dai et al., 2011; Wang et al., 2010;~~  
172 Du et al., 2020; Zhou et al., 2021).

域代码已更改

域代码已更改

域代码已更改

带格式的: 字体颜色: 自动设置

域代码已更改

173 Discontinuities are inevitably occurred in the long-term observation system which  
174 are required to be checked out and adjusted in the raw data. The homogenized series  
175 pose a significant role in realistic and reliable assessment of climate trend and  
176 variability. The main objective of this study is to detect and adjust the inhomogeneity  
177 in  $R_s$  estimates over Japan. The metadata were first extracted from website information  
178 and related records at each site. The SunDu observations were converted into  $R_s$ . The  
179 RHtest-QM method was applied to homogenize the observed  $R_s$  and SunDu-derived  $R_s$ ,  
180 and finally, the century-long homogenized ~~long term~~- $R_s$  data were ~~derived-produced~~

181 over Japan. Furthermore, the impacts of cloud cover and aerosols on  $R_s$  variation over  
182 Japan in recent decades were explored.

## 183 2. Data and methods

### 184 2.2.1 Surface incident solar radiation and sunshine duration

185 The monthly observed  $R_s$  at 105 stations and SunDu at 156 stations were  
186 downloaded from the Japanese Meteorology Agency (JMA) website (see Table S1 and  
187 Figure 1).  $R_s$  records were available from 1961. During the 1960s, two  $R_s$  measurements  
188 were conducted in parallel by both Eppley and Robitzsch pyranometers. In the early  
189 1970s (see Figure 2 and Table S2), these instruments were replaced by Moll-Gorczyński  
190 thermopile pyranometers. This replacement occurred at approximately 12.4% of  $R_s$   
191 stations in 1971, followed by ~~-2422.9%~~, ~~2624.8%~~, ~~43.8%~~ and ~~3230.5%~~ in the next four  
192 years, which may have caused severe data discontinuity problems (Tanaka et al., 2016).

193 SunDu has been routinely measured since 1890. Jordan recorders were replaced  
194 by EKO rotating mirror recorders at ~~nearly 5049.4%~~ of SunDu stations in 1986. ~~Before~~  
195 ~~Until~~ 1990, nearly all of the SunDu stations used new instruments for observations.  
196 ~~Less than 4.5%~~ of SunDu stations before 1985 and ~~more than 109.0%~~ of SunDu stations  
197 after 2000 were moved away from the original sites (see Figure 2 and Table S2)  
198 (Stanhill and Cohen, 2008).

199 In this study, SunDu was used to derive  $R_s$  based on the following equation (Yang

带格式的: 字体: (中文) 宋体

带格式的: 正文, 缩进: 首行缩进: 2 字符, 行距: 单倍行距

域代码已更改

域代码已更改

域代码已更改

201 et al., 2006):

$$202 \quad R_s / R_c = a_0 + a_1 \cdot n / N + a_2 \cdot (n / N)^2 \quad (1)$$

203 where  $n$  is sunshine duration hours;  $N$  is the maximum possible sunshine duration;  $R_c$   
204 is surface solar radiation under clear skies; and  $a_0$ ,  $a_1$  and  $a_2$  are coefficients. This  
205 method was recommended in many studies (Wang et al., 2015; Tang et al., 2011).

域代码已更改

206

带格式的: 字体颜色: 自动设置

207

## 208 2.2. Homogenization method

209 Both  $R_s$  and SunDu measurements over Japan suffer severe inhomogeneity  
210 problems, which require rigorous data homogenization. RHtest  
211 (<http://etccdi.pacificclimate.org/software.shtml>) is a widely used method to detect and  
212 adjust multiple changepoints in a climate data series, such as in surface temperature  
213 (Du et al., 2020), radiosonde temperature (Zhou et al., 2021), precipitation (Wang et al.,  
214 2010) and surface incident solar radiation (Yang et al., 2018). Two algorithms were  
215 provided to detect changepoints based on the penalized maximal T (PMT) test (Wang  
216 et al., 2007) and the penalized maximal F (PMF) test (Wang, 2008b). The problem of  
217 lag-1 autocorrelation in detecting mean shifts in time series was also resolved (Wang,  
218 2008a). The PMT algorithm requires the base time series to be no trend, and hence a  
219 reference series is needed. It is invalid when a reference series is not often available or  
220 its homogeneity is not sure, also the trend in the base and reference series are probably  
221 different. The PMF algorithm allows the time series in a constants trend and thus is

域代码已更改

域代码已更改

域代码已更改

域代码已更改

域代码已更改

域代码已更改

域代码已更改

222 applicable without a reference series. Both algorithms have higher detection power and  
223 the false alarm rate can be reduced by empirically constructed penalty function.

224 As the change of instrument in  $R_s$  and SunDu observation nearly happened  
225 nationwide and simultaneously, it is difficult to find reference data series to match the  
226 base data series and hence the PMF algorithm was used to detect the changepoints in  
227 this study. Multiple changepoints were detected including climate signals and artificial  
228 shifts, and only the ones confirmed by discontinuity information from metadata in Table  
229 S2 were left to be adjusted. Then two homogenized series based on direct measurement  
230 of  $R_s$  and SunDu-derived  $R_s$  were obtained.

231 Large uncertainties may still exist in both homogenized data series as the  
232 discontinuities in the raw observations may not be sufficiently and correctly recorded  
233 in the metadata. Further changepoints can be detected by considering the impact of the  
234 variation of independent climate variables such as clouds and aerosols on the  $R_s$   
235 variation. If these uncertainties were found, further changepoint detections were needed  
236 based on the PMT or PMF algorithm.

237 ~~As the discontinuity dates were recorded on the JMA websites, we artificially treat~~  
238 ~~these observations on those dates as changepoints.~~ To diminish all significant artificial  
239 shifts caused by the changepoints, a newly developed Quantile-Matching (QM)  
240 adjustments in the RHtest (Vincent et al., 2012; Wang et al., 2010) were performed to  
241 adjust the series so that the empirical distributions of all segments of the detrended base  
242 series agree with each other. The corrected values are all based on the empirical

域代码已更改

243 frequency of the datum to be adjusted.

244 Another independent homogenization method proposed by Katsuyama (1987),  
245 which was developed due to the replacement of the Jordan recorders with EKO rotating  
246 mirror recorder during the late 1980s, is denoted as follows:

$$247 \quad S_R = 0.8 S_J \quad (S_J < 2.5 \text{ h/day}) \quad (2)$$

$$248 \quad S_R = S_J - 0.5 \text{ h/day} \quad (S_J \geq 2.5 \text{ h/day}) \quad (3)$$

249 where  $S_J$  is the daily SunDu observed by the Jordan recorders before replacement; and  
250  $S_R$  is the daily SunDu adjusted to be consistent with the values observed with the EKO  
251 rotating mirror recorders.

252 These two homogenization methods were compared in this study and yielded  
253 nearly the same SunDu-derived  $R_s$  variation, as shown in Figure 3. Although the  
254 second method proposed by Katsuyama (1987) is simple and efficient, we just use it  
255 to cross validate the accuracy of the RHtest method. For the following analysis, the  
256 SunDu-derived  $R_s$  homogenized by RHtest was used as RHtest method provides  
257 higher power to detect the changepoints in a data series no matter the metadata are  
258 available. Since most artificial shifts in observation system were undocumented  
259 worldwide, the statistical methods including RHtest are optimal to identify these non-  
260 climatic signals and reduce the discontinuities in the data series.

### 261 2.3 Clouds

262 Clouds play an important role in  $R_s$  variation (Norris and Wild, 2009). Monthly  
263 cloud cover observations at 155 stations were also available on the JMA website. The

域代码已更改

域代码已更改

域代码已更改

264 observation time for cloud amount has been 08:00-19:00 since 1981 at ~~109.0%~~ of cloud  
 265 amount stations and 08:30-17:00 from 1990 to 1995 at another ~~1015.4%~~ of cloud  
 266 amount stations (see Figure 2 and Table S2). However, the difference between annual  
 267 raw and homogenized cloud data is trivial, as cloud data are relatively homogeneous in  
 268 space compared with  $R_s$  and SunDu observations. A site observation of cloud amount  
 269 can represent the value over a large spatial scale, likely leading to few inhomogeneity  
 270 issues for cloud data. ~~The Clouds and the Earth's Radiant Energy System (CERES)~~  
 271 ~~provides surface incident solar radiation (Ma et al., 2015) primarily based on the~~  
 272 ~~Moderate Resolution Imaging Spectroradiometer (MODIS) cloud and aerosol products~~  
 273 ~~(Kato et al., 2012).~~

带格式的: 字体颜色: 自动设置  
域代码已更改

带格式的: 字体颜色: 自动设置  
带格式的: 字体颜色: 自动设置

274 To explore the impact of the cloud cover anomaly on the  $R_s$  variation, the cloud  
 275 cover radiative effect (CCRE), defined as the change in  $R_s$  produced by a change in  
 276 cloud cover, was proposed by (Norris and Wild, 2009):

$$277 \quad CCRE'(lat, lon, y, m) = CC'(lat, lon, y, m) \times CRE(g, m) / \overline{CC}(g, m) \quad (4)$$

278 where  ~~$g$  is the grid lat is the latitude,  $lon$  is the longitude,  $y$  is the year,  $m$  is the~~  
 279 month,  $CCRE'$  is the cloud cover radiative effect anomaly,  $CC'$  is the cloud cover  
 280 anomaly,  $\overline{CC}$  is the ~~long term mean climatology of cloud cover in 12 months~~ and  $CRE$   
 281 is the cloud radiative effect calculated by the  $R_s$  difference under all sky and clear sky  
 282 conditions.

带格式的: 字体颜色: 自动设置  
带格式的: 字体颜色: 自动设置  
带格式的: 字体颜色: 自动设置  
带格式的: 字体颜色: 自动设置  
带格式的: 字体颜色: 自动设置  
带格式的: 字体颜色: 自动设置  
带格式的: 字体颜色: 自动设置  
带格式的: 字体颜色: 自动设置

283 The residual radiative effect was determined by removing the CCRE anomalies  
 284 from the  $R_s$  anomalies. It is noted that a part of the cloud albedo radiative effect

285 proportional to the cloud amount was contained in the CCRE, as a large cloud amount  
286 tends to yield enhanced cloud albedo, whereas another part of the cloud albedo radiative  
287 effect due to the aerosol first indirect effect (more aerosols facilitating more cloud  
288 condensation nuclei may enhance cloud albedo) may be included in the residual  
289 radiative effect, which mainly contains the aerosol radiative effect. ~~In this study, long-~~  
290 ~~term observations of cloud amount and monthly cloud radiative effect (CRE) data in~~  
291 ~~the CERES EBAF edition were used following Equation (4) to distinguish the cloud~~  
292 ~~cover radiative effect from Rs variation.~~

293 The Clouds and the Earth's Radiant Energy System (CERES) provides a reliable  
294 surface incident solar radiation (Ma et al., 2015) primarily based on the Moderate  
295 Resolution Imaging Spectroradiometer (MODIS) cloud and aerosol products (Kato et  
296 al., 2012). The cloud amount in CERES agrees well with the observations, and the  
297 annual CRE in CERES is well correlated with the annual cloud amount in Figure 10.  
298 The regional average cloud amount over Japan in Figure 10 (blue line) increases at a  
299 rate of 0.7% per decade from 1960 to 2015, which is consistent with the previous results  
300 (Figure 4 in Tsutsumi and Murakami (2012)).

301 In this study, long-term observations of cloud amount and monthly cloud radiative  
302 effect (CRE) data in the CERES EBAF edition were used following Equation (4) to  
303 distinguish the cloud cover radiative effect from Rs variation.

#### 304 **2.4 Data Processing**

305 We first interpolated the monthly observational data at sites into  $1^{\circ} \times 1^{\circ}$  grid data.

带格式的: 字体颜色: 自动设置

域代码已更改

带格式的: 字体颜色: 自动设置

带格式的: 字体颜色: 自动设置

域代码已更改

带格式的: 字体颜色: 自动设置

306 and then calculated the area average of the climate variables. As the brightening and  
307 dimming over Japan were the main concern in this study, monthly values were  
308 converted into annual values for calculation. If there are missing values in any month  
309 in a specific year, the annual value for that year is set to a missing value. The linear  
310 regression was used for trend calculation.

### 311 **3. Results**

312 In this section, we first compared the observed  $R_s$  and sunshine duration derived  
313  $R_s$  before and after adjustment to demonstrate the necessity and feasibility of the  
314 homogenization procedure in Section 3.1. As artificial shifts may not be sufficiently  
315 and correctly documented by metadata, uncertainties may still exist in the homogenized  
316 series. We then tried to explore these uncertainties by considering the influence of other  
317 independent climate variables such as clouds, aerosols on the  $R_s$  variation, and  
318 ultimately informed a more reasonable homogenized  $R_s$  series in Section 3.2. In Section  
319 3.3, we claimed the significant correction in trend analysis of  $R_s$  in Japan and quantified  
320 the influence of clouds and aerosols on the  $R_s$  variation.

#### 321 **3.1 Homogenization of observed $R_s$ and sunshine duration derived $R_s$**

322 ~~In this study, monthly values were converted into annual values for calculation.~~  
323 ~~If there are missing values in any month in a specific year, the annual value for that~~  
324 ~~year is set to a missing value. Both  $R_s$  and SunDu records are available at 105 stations.~~  
325 ~~Figure 4 shows the~~ The comparisons between raw data and homogenized data at each



326 site were shown in Figure 4 and their difference were illustrated in Figure 5.  
327 Compared with raw data, the absolute values of biases between  $R_s$  and SunDu-derived  
328  $R_s$  at 74 stations decrease after homogenization, of which the absolute values of biases  
329 decrease by more than  $4 \text{ W m}^{-2}$  at 42 stations and more than  $10 \text{ W m}^{-2}$  at 8 stations.  
330 The root mean square errors at 80 stations were reduced after homogenization, of  
331 which reduces are more than  $4 \text{ W m}^{-2}$  at 40 stations. After ~~QM~~-adjustments, the  
332 correlation coefficients between the annual observed  $R_s$  and annual SunDu-derived  $R_s$   
333 are improved at 68 stations, including greater than 0.2 improvement at 31 stations.  
334 significant with a 90% confidence interval at 75 stations. The correlation coefficients  
335 were improved at 54 of 75 stations after homogenization, including 31 stations that  
336 had improvements greater than 0.2. Among the 54 stations, there were are 41 stations  
337 (marked with red in Table S1, Figure 6) at which the correlation coefficients were  
338 greater than 0.5, and the biases and the root mean square errors generally decrease  
339 after homogenization.

340 Figure ~~57~~, as an example, shows the time series of surface incident solar  
341 radiation ( $R_s$  and SunDu-derived  $R_s$ ) at the HAMADA site (WMO-ID: 47755, Lat:  
342 34.9, Lon: 132.07) before and after homogenization. Details in the improvements  
343 after homogenization at most stations can be traced back to Figures 4, 5 and 6. The  
344 improved patterns of time series of surface incident solar radiation after  
345 homogenization ~~which~~ highlights the necessity and feasibility of the RHtest-~~QM~~  
346 method. The SunDu-derived  $R_s$  variation over Japan during recent decades inferred

347 from these “perfect” data at 41 sites (Figure 68) was nearly identical to that from all  
348 available data at 156 sites (as shown in Table 1 and Figure 79).

349 ~~The cloud amount in CERES agrees well with the observations, and the annual~~  
350 ~~CRE in CERES is well correlated with the annual cloud amount in Figure 8. The~~  
351 ~~regional average cloud amount over Japan in Figure 8 (blue line) increases at a rate of~~  
352 ~~0.7% per decade from 1960 to 2015, which is consistent with the results (Figure 4) in~~  
353 ~~(Tsutsumi and Murakami, 2012).~~

带格式的: 字体颜色: 自动设置

带格式的: 字体颜色: 自动设置

域代码已更改

### 354 3.2 Uncertainties in $R_s$ observations

355 Figure 7-9 displays the change in  $R_s$  during the last 5 decades, while Figure 8-10  
356 shows the variation in observed clouds over Japan. The sharp decrease in  $R_s$  in 1963  
357 ~~was attributed to caused by~~ the volcanic eruption of Agung in Indonesia ~~in the same year~~  
358 ~~(Witham, 2005) can be clearly found.~~ The sharp decreases in  $R_s$  in 1991 and 1993 are  
359 due to the combined effect of the volcanic eruption of Mount Pinatubo in the Philippines  
360 in 1991 ~~(Robock, 2000) and the simultaneous significant increases in clouds (shown in~~  
361 ~~(Figure 8) in~~ Tsutsumi and Murakami (2012)). The volcanic eruption of El Chichón in  
362 Mexico in 1982 exerted little impact on the decline in  $R_s$  and may have been  
363 compensated by the decrease in clouds, as shown in Figure 8-10. The pronounced  $R_s$   
364 decline in 1980 coincides with the significant increase in clouds, while the lightening  
365 of  $R_s$  in 1978 and 1994 encounters abrupt decreases in cloud covers.

域代码已更改

域代码已更改

域代码已更改

366 As shown in Figure 79, ~~no major modifications were found in~~  $R_s$  observations  
367 ~~before and change little~~ after homogenization (comparison between the light blue and

368 dark blue lines). However, the SunDu-derived  $R_s$  series are smoother after adjustment  
369 by the QM method, as the sharp decrease from 1983 to 1993 caused by the replacement  
370 of sunshine duration instruments (Jordan recorders were replaced with EKO rotating  
371 mirror recorders) (Stanhill and Cohen, 2008) was repaired (comparison between the  
372 light red line and dark red lines). Despite the identical increase in  $R_s$  via both the  
373 homogenized direct measurements of  $R_s$  and the homogenized SunDu-derived  $R_s$  during  
374 the 1995-2014 period, their variations in  $R_s$  from 1961 to 1994 are different (dark red  
375 line and dark blue line).

域代码已更改

376 Large discrepancies in  $R_s$  variation were found during the time period of 1961-  
377 1970, although homogenizations were performed on the direct measurements of  $R_s$  and  
378 SunDu-derived  $R_s$  (dark blue line and dark red line in Figure 79). Existing study noted  
379 the inaccurate instruments used at the beginning of operation ~~of~~in the  $R_s$  observation  
380 network in approximately 1961, and the parallel use of two different types of  
381 instruments during the 1960s may result in the large variability in observed  $R_s$  (Tanaka  
382 et al., 2016). At this time, the clouds fluctuated gently, as shown in Figure 810, and the  
383 change in volcanic aerosols from 1965 to 1966 was nearly the same as that from 1962  
384 to 1963 (Table 2 in Sato et al. (1993)), so the sudden decline in the direct observations  
385 of  $R_s$  from 1965 to 1966, which was twice as large as that from 1962 to 1963, is  
386 suspicious. It is inferred that anthropogenic aerosols play a subtle role in the significant  
387 reduction in  $R_s$ , as this type of phenomenon is common for both polluted and pristine  
388 stations in Japan (Figure 22 in Tanaka et al., 2016).

域代码已更改

域代码已更改

域代码已更改

389 Figure 9-11 shows the correlation coefficients between homogenized  $R_s$  (observed  
390 and SunDu-derived) and cloud amount. In general, the observed  $R_s$  (-0.45) is less  
391 correlated than the SunDu-derived  $R_s$  (-0.67), particularly from 1961 to 1970, -0.21  
392 compared with -0.64. This in turn supports the reliability of homogenized SunDu-  
393 derived  $R_s$ , especially during the time period of 1961-1970. The ~~misleading-false~~  
394 ~~variability of the observed  $R_s$  variation from 1961 to 1970~~ was modified by the RHtest  
395 method against ~~using the~~ homogenized SunDu-derived  $R_s$  ~~as reference data from 1961~~  
396 ~~to 1970~~ as shown in Figure 4-12.

397 General decreases in stratospheric aerosol optical depth (AOD) were reported in  
398 Sato et al. (1993) from 1965 to 1980, and clouds fluctuated slightly, as shown in Figure  
399 8-10; both of these factors contributed to a brightening of  $R_s$ . This is in agreement with  
400 the SunDu-derived  $R_s$  and contrasts with the direct measurements of  $R_s$ .

401 During the 1985-1990 period, clouds varied slightly, as shown in Figure 8-10, and  
402 the observed atmospheric transmission under cloud-free conditions increased (Wild et  
403 al., 2005), which suggests that the large declines in directly observed  $R_s$  and SunDu-  
404 derived  $R_s$  are defective and reinforce the reliability of the adjusted SunDu-derived  $R_s$   
405 (dark red line in Figure 7-9).

406 From the above analysis, it can be inferred that fewer uncertainties exist in  
407 homogenized SunDu-derived  $R_s$ , which was confirmed by another work that utilized a  
408 different data adjusted method (Stanhill and Cohen, 2008). ~~However, quantifying the~~  
409 ~~accuracy of homogenized SunDu-derived  $R_s$  seems not to be accessible until more~~  
410 ~~accurate observations of  $R_s$  are available.~~

域代码已更改

域代码已更改

域代码已更改

411 **3.2 Trends of  $R_s$  over Japan**

412 The trends of  $R_s$  during specific time periods for different types of datasets are  
413 listed in Table 1. Direct measurements of  $R_s$  and SunDu-derived  $R_s$  from 41 selected  
414 stations and all available stations reveal similar variations in  $R_s$  over Japan, which  
415 demonstrates that the sample number has a subtle impact on the estimation of global  
416 brightening and dimming over Japan.

417 A revisit of global dimming and brightening was list in Table 1. Major-Major  
418 differences were found in the time periods of 1961-1980, ranging from -11.2 (-12.0) to  
419 -8.4 (-4.8)  $W m^{-2}$  per decade before and after  $R_s$  homogenizations for all available  
420 stations (41 selected stations) over Japan. ~~In addition,~~ significant repairs occurred  
421 during the 1981-1995 period, ranging from -10.6 (-11.3) to -1.2 (-1.3)  $W m^{-2}$  per decade  
422 before and after SunDu-derived  $R_s$  homogenizations for all available stations (41  
423 selected stations) over Japan. Both corrections were mainly attributed to the  
424 homogenization of corrupted raw data caused by the replacement of instruments for  $R_s$   
425 and SunDu measurements. After careful checking and adjustment of the SunDu-derived  
426  $R_s$  series, the decadal variation in  $R_s$  over Japan, which was totally different from former  
427 studies (Wild et al., 2005; Norris and Wild, 2009), was remedied. Direct measurements  
428 of  $R_s$  display nearly zero trend from 1961 to 2014 over Japan, while their  
429 homogenization series report a positive change of 0.8-1.6  $W m^{-2}$  per decade; SunDu-  
430 derived  $R_s$  decrease at a rate of 1.9  $W m^{-2}$  per decade, while its homogenized series  
431 reveals a brightening of 0.9  $W m^{-2}$  per decade.

域代码已更改

432 The combined effects of clouds and aerosols on  $R_s$  make the global dimming and  
433 brightening complicated. The CCRE can explain 70% of global brightening from 1961  
434 to 2014 at monthly and interannual time scales, while the residual radiative effect  
435 dominates the decadal variation in  $R_s$ , as shown in Figure 13 and Table 1, which is in  
436 agreement with Wang et al. (2012). Homogenized SunDu-derived  $R_s$  show an increase  
437 of  $1.6 \text{ W m}^{-2}$  per decade from 1961 to 1980; however, persistent increase in cloud  
438 amount yields a CCRE decrease of  $1.1 \text{ W m}^{-2}$  per decade. The residual radiative effect  
439 accounts for an increase of  $2.4 \text{ W m}^{-2}$  per decade for this time period. The cloud  
440 radiative effect ( $-1.4 \text{ W m}^{-2}$  per decade) modulates  $R_s$  variation of  $-1.2 \text{ W m}^{-2}$  per decade  
441 for the 1981-1995 period, while the residual radiative effect ( $1.2 \text{ W m}^{-2}$  per decade)  
442 dominates  $R_s$  variation of  $1.4 \text{ W m}^{-2}$  per decade from 1996 to 2014.

域代码已更改

443 Homogenized SunDu-derived  $R_s$  shows a slight increase of  $0.9 \text{ W m}^{-2}$  per decade  
444 from 1961 to 2014 with a 90% confidence interval. However, the CCRE accounts for a  
445 decreased  $R_s$  of  $1.4 \text{ W m}^{-2}$  per decade, which implies that cloud cover changes are not  
446 the primary driving forces for the  $R_s$  trend over Japan. Meanwhile, the residual radiative  
447 effect exhibits an increase of  $2.2 \text{ W m}^{-2}$  per decade, which surpasses the negative CCRE.

448 Several studies demonstrate a generally cleaner sky over Japan from the 1960s to  
449 the 2000s (except for the years impacted by volcanic eruptions) based on atmospheric  
450 transparency and aerosol optical properties (Wild et al., 2005; Kudo et al., 2012), which  
451 supports the dominant role of aerosols in  $R_s$  brightening over Japan, as revealed by the  
452 residual radiative effect here. Furthermore, the residual radiative effect in this study is

域代码已更改

453 stronger than that in [Norris and Wild \(2009\)](#), as raw data were remedied and more  
454 accurate satellite data from CERES were adopted to quantify the radiative effect.  
455 [Tsutsumi and Murakami \(2012\)](#) demonstrated that cloud amount categories exert an  
456 important effect on  $R_s$  variation.  $R_s$  enhancement by the increased appearance of large  
457 cloud amounts is superior to  $R_s$  decline by the decreased appearance of small cloud  
458 amounts during 1961-2014, which yields increased  $R_s$  with increasing total cloud  
459 amount. They also pointed out that the decrease in cloud optical thickness due to the  
460 large emissions of SO<sub>2</sub> and black carbon from East Asia through the aerosol semi-direct  
461 effect (absorption of more energy by aerosols results in the evaporation or suppression  
462 of clouds) may have facilitated the increased  $R_s$  over Japan.

域代码已更改

域代码已更改

域代码已更改

463 The decrease in spring dust storms in March-May during the last 5 decades from  
464 China ([Qian et al., 2002](#); [Zhu et al., 2008](#)), which may travel to neighboring  
465 countries([Uno et al., 2008](#); [Choi et al., 2001](#)), could also have triggered the increase in  
466  $R_s$  over Japan. The  $R_s$  variation and radiative effect in different seasons are categorized  
467 in Figure 142 and Table 2, in which an increasing trend of 1.5 W m<sup>-2</sup> per decade in the  
468 homogenized SunDu-derived  $R_s$  prevails in spring for the whole time period, dominated  
469 by a dramatic increase of 2.8 W m<sup>-2</sup> per decade in the residual effect and even larger  
470 increase ~~during-for~~ 1961-1980 (3.1 W m<sup>-2</sup> per decade) and 1996-2014 (3.4 W m<sup>-2</sup> per  
471 decade).

域代码已更改

域代码已更改

#### 472 4. Data availability

473 Monthly observed surface incident solar radiation, sunshine duration and cloud  
474 amount data were provided by Japan Meteorological Agency  
475 (<https://www.data.jma.go.jp/obd/stats/data/en/smp/index.html>), and monthly cloud  
476 radiative effect (CRE) data were derived from Clouds and the Earth's Radiant Energy  
477 System for CERES EBAF data ([https://ceres.larc.nasa.gov/order\\_data.php](https://ceres.larc.nasa.gov/order_data.php)). The  
478 homogenized observed  $R_s$  and SunDu-derived  $R_s$  used in this study are available at  
479 <https://doi.org/10.11888/Meteoro.tpsc.271524> (Ma et al., 2021).

#### 480 5. Conclusions

481 The homogenization of raw observations related to  $R_s$  can significantly improve  
482 the accuracy of global dimming and brightening estimation and provide a reliable  
483 assessment of climate trends and variability. ~~Observational data themselves have~~  
484 ~~inherent problems caused by measurement method, instrument replacement and site~~  
485 ~~relocation. Therefore, precautions should be taken when using these data for trend~~  
486 ~~analysis or as validation data.~~ In this study, we for the first time the RHtest-QM method  
487 ~~was introduced to homogenize the direct measurements of raw  $R_s$  and SunDu-derived~~  
488  ~~$R_s$  observation over Japan using the information in metadata as changepoints and~~  
489 ~~obtained a more reliable  $R_s$  data series over Japan for century-long.~~

490 Documented artificial shifts in metadata play an important role in regulating the

带格式的: 字体颜色: 自动设置

带格式的: 字体颜色: 自动设置

带格式的: 字体颜色: 自动设置

域代码已更改

带格式的: 字体颜色: 自动设置

域代码已更改

带格式的: 字体颜色: 自动设置

带格式的: 字体颜色: 自动设置

带格式的: 字体颜色: 自动设置

带格式的: 字体颜色: 自动设置

带格式的: 字体颜色: 自动设置



491 raw observations. If changepoints were confirmed by metadata or other independent  
492 climate variables, RHtest method was applied to remove the discontinuities. In this  
493 study, ~~Inhomogeneities shifts~~ in the homogenized raw  $R_s$  ~~was were~~ further checked by  
494 exploring the relationship with the ground-based cloud amount and tuned again using  
495 homogenized SunDu-derived  $R_s$  as the reference data. By comparing the variations in  
496 independent climate variables of cloud and aerosol, the homogenized SunDu-derived  
497  $R_s$  were proved to be more reliable in detecting  $R_s$  variability over Japan.

带格式的: 字体颜色: 自动设置

带格式的: 字体颜色: 自动设置

498 A revisit of global dimming and brightening is made based on the homogenized  
499  $R_s$  series. The global dimming and brightening over Japan were revisited based on the  
500 homogenized SunDu derived  $R_s$ , which diminished the effect of nonclimate signals in  
501 the raw observations.

带格式的: 字体颜色: 自动设置

带格式的: 字体颜色: 自动设置

502  $R_s$  over Japan increases at a rate of  $1.6 \text{ W m}^{-2}$  per decade for 1961-1980, which is  
503 contrary to the trend ( $-4.8 \sim -12.0 \text{ W m}^{-2}$  per decade) in the unreasonable  $R_s$  observation.  
504 A slight decrease of  $1.2 \text{ W m}^{-2}$  per decade for 1981-1995 in homogenized SunDu-  
505 derived  $R_s$  accounts for only 1/10 of the trend in its unadjusted series. This directly  
506 contributes a brightening of  $0.9 \text{ W m}^{-2}$  per decade (with a 99% confidence interval) for  
507 the last 5 decade in homogenized series, which is totally contrary to the variation in its  
508 original series. experienced a sudden decline in  $R_s$  in 1963, a global brightening of  $4.8$   
509  $\text{W m}^{-2}$  per decade ( $P < 0.01$ ) from 1963 to 1977, a rapid increase in 1978, a sudden  
510 decrease in 1980, a global dimming of  $5.1 \text{ W m}^{-2}$  per decade ( $P < 0.10$ ) from 1981 to  
511 1993, a pronounced increase in 1994, and a nearly  $1 \text{ W m}^{-2}$  per decade increase from

带格式的: 字体: (中文) + 中文正文 (宋体)

带格式的: 字体颜色: 自动设置

带格式的: 字体颜色: 自动设置

带格式的: 字体颜色: 自动设置

512 1995 to 2014. For the last 5 decades, a slight global brightening of  $1 \text{ W m}^{-2}$  per decade  
513 (with a 99% confidence interval) was inferred from the homogenized SunDu derived  
514  $R_s$ . Global brightening since 1961 over Japan is consistent with that in Stanhill and  
515 Cohen (2008), except that the magnitude is not as large.

带格式的: 字体颜色: 自动设置

516 We also explored how the clouds and aerosols are the two major factors that  
517 mediate the transformation of  $R_s$ . The brightening in Japan for 1961-1980 was the  
518 combined effect of cloud cover (negative effect) and aerosols (positive effect). The  
519 dimming for 1981-1995 was governed by reduced cloud amounts, while the increase in  
520  $R_s$  for 1996-2014 was controlled by decreased aerosols. These results are different  
521 from those in Norris and Wild (2009), as homogenization was performed on the raw  
522 data and more accurate cloud radiative effect data series from CERES were utilized in  
523 our study. During the entire period of 1961-2014, cloud amounts dominated seasonal  
524 and interannual  $R_s$  variations, while aerosols (including aerosol-cloud interactions)  
525 drove decadal  $R_s$  variations over Japan, noted by other studies, in response to  
526 generally cleaner skies and a reduction in spring Asian dust storms (Wang et al., 2012;  
527 Kudo et al., 2012).

域代码已更改

域代码已更改

域代码已更改

域代码已更改

528 \_\_\_\_\_

529 **Author contributions**

530 QM and KW designed the research and wrote the paper. LS collected the raw data. YH  
531 homogenized the raw data. QW provided the technical support. YZ and HL checked the  
532 data.

533

534 **Competing interests**

535 The authors declare that they have no conflict of interest.

536

537

538

539

### **Acknowledgements**

540 This study is funded by the National Key R&D Program of China (2017YFA0603601),

541 the National Science Foundation of China (41930970), and Project Supported by State

542 Key Laboratory of Earth Surface Processes and Resource Ecology (2017-KF-03). We

543 thank many institutions for sharing their data: Japan Meteorological Agency for

544 observation data over Japan

545 (<https://www.data.jma.go.jp/obd/stats/data/en/smp/index.html>); Clouds and the Earth's

546 Radiant Energy System for CERES EBAF data

547 ([https://ceres.larc.nasa.gov/order\\_data.php](https://ceres.larc.nasa.gov/order_data.php)). We thank the Expert Team on Climate

548 Change Detection and Indices (ETCCDI) for providing the RHtestV4 homogenization

549 package (<http://etccdi.pacificclimate.org/software.shtml>).

550

551

553 **References**

- 554 Aguilar, E., Auer, I., Brunet, M., Peterson, T. C., and Wieringa, J.: Guidelines on  
 555 climate metadata and homogenization, WMO-TD No. 1186, 1186, 2003.
- 556 Alexandersson, H.: A homogeneity test applied to precipitation data, 6, 661-675,  
 557 <https://doi.org/10.1002/joc.3370060607>, 1986.
- 558 Allen, R. J., Norris, J. R., and Wild, M.: Evaluation of multidecadal variability in  
 559 CMIP5 surface solar radiation and inferred underestimation of aerosol direct effects  
 560 over Europe, China, Japan, and India, *J Geophys Res-Atmos*, 118, 6311-6336,  
 561 10.1002/jgrd.50426, 2013.
- 562 Augustine, J. A. and Hodges, G. B.: Variability of Surface Radiation Budget  
 563 Components Over the U.S. From 1996 to 2019—Has Brightening Ceased?, 126,  
 564 e2020JD033590, <https://doi.org/10.1029/2020JD033590>, 2021.
- 565 Choi, J. C., Lee, M., Chun, Y., Kim, J., and Oh, S.: Chemical composition and source  
 566 signature of spring aerosol in Seoul, Korea, *J Geophys Res-Atmos*, 106, 18067-  
 567 18074, <https://doi.org/10.1029/2001JD900090>, 2001.
- 568 Dai, A., Wang, J., Thorne, P. W., Parker, D. E., Haimberger, L., and Wang, X. L.: A  
 569 New Approach to Homogenize Daily Radiosonde Humidity Data, *J Climate*, 24, 965-  
 570 991, 10.1175/2010jcli3816.1, 2011.
- 571 Du, J., Wang, K., Cui, B., and Jiang, S.: Correction of Inhomogeneities in Observed  
 572 Land Surface Temperatures over China, *J Climate*, 33, 8885-8902, 10.1175/jcli-d-19-  
 573 0521.1, 2020.
- 574 Dwyer, J. G., Norris, J. R., and Ruckstuhl, C.: Do climate models reproduce observed  
 575 solar dimming and brightening over China and Japan?, *J Geophys Res-Atmos*, 115,  
 576 <https://doi.org/10.1029/2009JD012945>, 2010.
- 577 Feng, F. and Wang, K.: Merging ground-based sunshine duration observations with  
 578 satellite cloud and aerosol retrievals to produce high-resolution long-term surface  
 579 solar radiation over China, *Earth Syst. Sci. Data*, 13, 907-922, 10.5194/essd-13-907-  
 580 2021, 2021a.
- 581 Feng, F. and Wang, K.: Merging High-Resolution Satellite Surface Radiation Data  
 582 with Meteorological Sunshine Duration Observations over China from 1983 to 2017,  
 583 *Remote Sens*, 13, 602, <https://doi.org/10.3390/rs13040602>, 2021b.
- 584 He, Y., Wang, K., Zhou, C., and Wild, M.: A Revisit of Global Dimming and  
 585 Brightening Based on the Sunshine Duration, 45, 4281-4289,  
 586 <https://doi.org/10.1029/2018GL077424>, 2018.
- 587 Inoue, T. and Matsumoto, J.: Seasonal and secular variations of sunshine duration and  
 588 natural seasons in Japan, *Int J Climatol*, 23, 1219-1234, 10.1002/joc.933, 2003.
- 589 Kato, S., Loeb, N. G., Rose, F. G., Doelling, D. R., Rutan, D. A., Caldwell, T. E., Yu,  
 590 L., and Weller, R. A.: Surface Irradiances Consistent with CERES-Derived Top-of-

域代码已更改

591 Atmosphere Shortwave and Longwave Irradiances, *J Climate*, 26, 2719-2740,  
592 10.1175/jcli-d-12-00436.1, 2012.

593 Katsuyama, M.: On comparison between rotating mirror sunshine recorders and  
594 Jordan sunshine recorders, *Weather Service Bulletin*, 54, 169-183, 1987.

595 Kudo, R., Uchiyama, A., Ijima, O., Ohkawara, N., and Ohta, S.: Aerosol impact on the  
596 brightening in Japan, *J Geophys Res-Atmos*, 117,  
597 <https://doi.org/10.1029/2011JD017158>, 2012.

598 Ma, Q., Wang, K. C., and Wild, M.: Impact of geolocations of validation data on the  
599 evaluation of surface incident shortwave radiation from Earth System Models, *J*  
600 *Geophys Res-Atmos*, 120, 6825-6844, 10.1002/2014JD022572, 2015.

601 Ma, Q., He, Y., Wang, K., and Su, L.: Homogenized solar radiation data set over  
602 Japan (1870-2015), National Tibetan Plateau Data Center [dataset],  
603 10.11888/Meteoro.tpcdc.271524, 2021.

604 Manara, V., Brunetti, M., Maugeri, M., Sanchez-Lorenzo, A., and Wild, M.: Sunshine  
605 duration and global radiation trends in Italy (1959–2013): To what extent do they  
606 agree?, 122, 4312-4331, <https://doi.org/10.1002/2016JD026374>, 2017.

607 Manara, V., Brunetti, M., Celozzi, A., Maugeri, M., Sanchez-Lorenzo, A., and Wild,  
608 M.: Detection of dimming/brightening in Italy from homogenized all-sky and clear-  
609 sky surface solar radiation records and underlying causes (1959–2013), *Atmos Chem*  
610 *Phys*, 16, 11145-11161, 10.5194/acp-16-11145-2016, 2016.

611 Manara, V., Beltrano, M. C., Brunetti, M., Maugeri, M., Sanchez-Lorenzo, A.,  
612 Simolo, C., and Sorrenti, S.: Sunshine duration variability and trends in Italy from  
613 homogenized instrumental time series (1936–2013), *J Geophys Res-Atmos*, 120,  
614 3622-3641, <https://doi.org/10.1002/2014JD022560>, 2015.

615 Noguchi, Y.: Solar radiation and sunshine duration in East Asia, *Archives for*  
616 *meteorology, geophysics, and bioclimatology, Series B*, 29, 111-128,  
617 10.1007/BF02278195, 1981.

618 Norris, J. R. and Wild, M.: Trends in aerosol radiative effects over China and Japan  
619 inferred from observed cloud cover, solar “dimming,” and solar “brightening”, *J*  
620 *Geophys Res-Atmos*, 114, <https://doi.org/10.1029/2008JD011378>, 2009.

621 Ohmura, A.: Observed decadal variations in surface solar radiation and their causes, *J*  
622 *Geophys Res-Atmos*, 114, <https://doi.org/10.1029/2008JD011290>, 2009.

623 Qian, W., Quan, L., and Shi, S.: Variations of the Dust Storm in China and its Climatic  
624 Control, *J Climate*, 15, 1216-1229, 10.1175/1520-  
625 0442(2002)015<1216:Votdsi>2.0.Co;2, 2002.

626 Qian, Y., Kaiser, D. P., Leung, L. R., and Xu, M.: More frequent cloud-free sky and  
627 less surface solar radiation in China from 1955 to 2000, *Geophys Res Lett*, 33, Artn  
628 L01812  
629 Doi 10.1029/2005gl024586, 2006.

630 Reeves, J., Chen, J., Wang, X. L., Lund, R., and Lu, Q. Q.: A Review and Comparison  
631 of Change-point Detection Techniques for Climate Data %J *Journal of Applied*

632 Meteorology and Climatology, 46, 900-915, 10.1175/jam2493.1, 2007.  
633 Robock, A.: Volcanic eruptions and climate, *Rev Geophys*, 38, 191-219,  
634 <https://doi.org/10.1029/1998RG000054>, 2000.  
635 Sanchez-Lorenzo, A. and Wild, M.: Decadal variations in estimated surface solar  
636 radiation over Switzerland since the late 19th century, *Atmos Chem Phys*, 12, 8635-  
637 8644, 10.5194/acp-12-8635-2012, 2012.  
638 Sanchez-Lorenzo, A., Calbó, J., and Martin-Vide, J.: Spatial and Temporal Trends in  
639 Sunshine Duration over Western Europe (1938–2004), *J Climate*, 21, 6089-6098,  
640 10.1175/2008jcli2442.1, 2008.  
641 Sanchez-Lorenzo, A., Calbó, J., and Wild, M.: Global and diffuse solar radiation in  
642 Spain: Building a homogeneous dataset and assessing their trends, *Global Planet*  
643 *Change*, 100, 343-352, <https://doi.org/10.1016/j.gloplacha.2012.11.010>, 2013.  
644 Sanchez-Lorenzo, A., Brunetti, M., Calbó, J., and Martin-Vide, J.: Recent spatial and  
645 temporal variability and trends of sunshine duration over the Iberian Peninsula from a  
646 homogenized data set, *J Geophys Res-Atmos*, 112,  
647 <https://doi.org/10.1029/2007JD008677>, 2007.  
648 Sanchez-Lorenzo, A., Wild, M., Brunetti, M., Guijarro, J. A., Hakuba, M. Z., Calbó,  
649 J., Mystakidis, S., and Bartok, B.: Reassessment and update of long-term trends in  
650 downward surface shortwave radiation over Europe (1939–2012), *J Geophys Res-*  
651 *Atmos*, 120, 9555-9569, <https://doi.org/10.1002/2015JD023321>, 2015.  
652 Sato, M., Hansen, J. E., McCormick, M. P., and Pollack, J. B.: Stratospheric aerosol  
653 optical depths, 1850–1990, *J Geophys Res-Atmos*, 98, 22987-22994,  
654 <https://doi.org/10.1029/93JD02553>, 1993.  
655 Shi, G. Y., Hayasaka, T., Ohmura, A., Chen, Z. H., Wang, B., Zhao, J. Q., Che, H. Z.,  
656 and Xu, L.: Data quality assessment and the long-term trend of ground solar radiation  
657 in China, *J Appl Meteorol Clim*, 47, 1006-1016, Doi 10.1175/2007jamc1493.1, 2008.  
658 Stanhill, G. and Cohen, S.: Solar Radiation Changes in the United States during the  
659 Twentieth Century: Evidence from Sunshine Duration Measurements, *J Climate*, 18,  
660 1503-1512, 10.1175/jcli3354.1, 2005.  
661 Stanhill, G. and Cohen, S.: Solar Radiation Changes in Japan during the 20th Century:  
662 Evidence from Sunshine Duration Measurements, *J Meteorol Soc Jpn. Ser. II*, 86, 57-  
663 67, 10.2151/jmsj.86.57, 2008.  
664 Tanaka, K., Ohmura, A., Folini, D., Wild, M., and Ohkawara, N.: Is global dimming  
665 and brightening in Japan limited to urban areas?, *Atmospheric Chemistry And*  
666 *Physics*, 16, 13969-14001, 10.5194/acp-16-13969-2016, 2016.  
667 Tang, W. J., Yang, K., Qin, J., Cheng, C. C. K., and He, J.: Solar radiation trend across  
668 China in recent decades: a revisit with quality-controlled data, *Atmos Chem Phys*, 11,  
669 393-406, 10.5194/acp-11-393-2011, 2011.  
670 Tsutsumi, Y. and Murakami, S.: Increase in Global Solar Radiation with Total Cloud  
671 Amount from 33 Years Observations in Japan, *J Meteorol Soc Jpn*, 90, 575-581,  
672 10.2151/jmsj.2012-409, 2012.

673 Uno, I., Yumimoto, K., Shimizu, A., Hara, Y., Sugimoto, N., Wang, Z., Liu, Z., and  
674 Winker, D. M.: 3D structure of Asian dust transport revealed by CALIPSO lidar and a  
675 4DVAR dust model, *Geophys Res Lett*, 35, <https://doi.org/10.1029/2007GL032329>,  
676 2008.

677 Vincent, L. A., Wang, X. L., Milewska, E. J., Wan, H., Yang, F., and Swail, V.: A  
678 second generation of homogenized Canadian monthly surface air temperature for  
679 climate trend analysis, *J Geophys Res-Atmos*, 117,  
680 <https://doi.org/10.1029/2012JD017859>, 2012.

681 Wang, K. C., Dickinson, R. E., Wild, M., and Liang, S.: Atmospheric impacts on  
682 climatic variability of surface incident solar radiation, *Atmos Chem Phys*, 12, 9581-  
683 9592, 10.5194/acp-12-9581-2012, 2012.

684 Wang, K. C., Ma, Q., Li, Z. J., and Wang, J. K.: Decadal variability of surface incident  
685 solar radiation over China: Observations, satellite retrievals, and reanalyses, *J*  
686 *Geophys Res-Atmos*, 120, 6500-6514, 10.1002/2015JD023420, 2015.

687 Wang, K. C., Dickinson, R. E., Ma, Q., Augustine, J. A., and Wild, M.: Measurement  
688 Methods Affect the Observed Global Dimming and Brightening, *J Climate*, 26, 4112-  
689 4120, 10.1175/Jcli-D-12-00482.1, 2013.

690 Wang, X. L.: Comments on "Detection of Undocumented Change-points: A Revision  
691 of the Two-Phase Regression Model" %J *Journal of Climate*, 16, 3383-3385,  
692 10.1175/1520-0442(2003)016<3383:Codouc>2.0.Co;2, 2003.

693 Wang, X. L.: Accounting for Autocorrelation in Detecting Mean Shifts in Climate  
694 Data Series Using the Penalized Maximal t or F Test, *J Appl Meteorol Clim*, 47, 2423-  
695 2444, 10.1175/2008jamc1741.1, 2008a.

696 Wang, X. L., Wen, Q. H., and Wu, Y.: Penalized Maximal t Test for Detecting  
697 Undocumented Mean Change in Climate Data Series, *J Appl Meteorol Clim*, 46, 916-  
698 931, 10.1175/jam2504.1, 2007.

699 Wang, X. L. L.: Penalized maximal F test for detecting undocumented mean shift  
700 without trend change, *J Atmos Ocean Technol*, 25, 368-384,  
701 10.1175/2007JTECHA982.1, 2008b.

702 Wang, X. L. L., Chen, H. F., Wu, Y. H., Feng, Y., and Pu, Q. A.: New Techniques for  
703 the Detection and Adjustment of Shifts in Daily Precipitation Data Series, *J Appl*  
704 *Meteorol Clim*, 49, 2416-2436, 10.1175/2010JAMC2376.1, 2010.

705 Wild, M. and Schmucki, E.: Assessment of global dimming and brightening in IPCC-  
706 AR4/CMIP3 models and ERA40, *Clim Dynam*, 37, 1671-1688, 10.1007/s00382-010-  
707 0939-3, 2011.

708 Wild, M., Wacker, S., Yang, S., and Sanchez-Lorenzo, A.: Evidence for Clear-Sky  
709 Dimming and Brightening in Central Europe, 48, e2020GL092216,  
710 <https://doi.org/10.1029/2020GL092216>, 2021.

711 Wild, M., Gilgen, H., Roesch, A., Ohmura, A., Long, C. N., Dutton, E. G., Forgan, B.,  
712 Kallis, A., Russak, V., and Tsvetkov, A.: From Dimming to Brightening: Decadal  
713 Changes in Solar Radiation at Earth's Surface, *Science*, 308, 847-850,



714 10.1126/science.1103215, 2005.  
715 Witham, C. S.: Volcanic disasters and incidents: A new database, *J Volcanol Geoth*  
716 *Res*, 148, 191-233, 10.1016/j.jvolgeores.2005.04.017, 2005.  
717 Xia, X.: A closer looking at dimming and brightening in China during 1961-2005,  
718 *Ann Geophys*, 28, 1121-1132, 10.5194/angeo-28-1121-2010, 2010.  
719 Yang, K., Koike, T., and Ye, B. S.: Improving estimation of hourly, daily, and monthly  
720 solar radiation by importing global data sets, *Agr Forest Meteorol*, 137, 43-55,  
721 10.1016/j.agrformet.2006.02.001, 2006.  
722 Yang, S., Wang, X. L., and Wild, M.: Homogenization and Trend Analysis of the  
723 1958–2016 In Situ Surface Solar Radiation Records in China, *J Clim*, 31, 4529-4541,  
724 10.1175/jcli-d-17-0891.1, 2018.  
725 Zeng, Z., Wang, Z., Gui, K., Yan, X., Gao, M., Luo, M., Geng, H., Liao, T., Li, X.,  
726 An, J., Liu, H., He, C., Ning, G., and Yang, Y.: Daily Global Solar Radiation in China  
727 Estimated From High-Density Meteorological Observations: A Random Forest Model  
728 Framework, 7, e2019EA001058, <https://doi.org/10.1029/2019EA001058>, 2020.  
729 Zhou, C., Wang, J., Dai, A., and Thorne, P. W.: A New Approach to Homogenize  
730 Global Subdaily Radiosonde Temperature Data from 1958 to 2018, *J Climate*, 34,  
731 1163-1183, 10.1175/jcli-d-20-0352.1, 2021.  
732 Zhu, C., Wang, B., and Qian, W.: Why do dust storms decrease in northern China  
733 concurrently with the recent global warming?, *Geophys Res Lett*, 35,  
734 <https://doi.org/10.1029/2008GL034886>, 2008.  
735  
736

737 Table 1. Trends of Surface Incident Solar Radiation ( $R_s$ ) in Japan during Specific Time  
 738 Periods for Different Types of Datasets<sup>a</sup>. Unit: W m<sup>-2</sup> per decade  
 739

Case <sup>b</sup>	Datasets <sup>c</sup>	1961-1980	1981-1995	1996-2014	1961-2014
Selected 41 Stations	OBS-raw	-12.0**	-2.1	2.4	-0.3
	OBS_HM	-4.8*	-2.1	2.4	1.5**
	OBS_2HM	-0.8*	-2.1	2.4*	0.9**
	SunDu-derived	1.4	-11.3**	1.4	-2.1**
	SunDu-derived_HM	1.4	-1.3*	1.5	0.9**
All Stations	OBS-raw	-11.2**	-1.3	2.2	0.2
	OBS_HM	-8.4**	-1.3	2.2	0.8
	OBS_2HM	0.7	-1.3	2.2	1.6**
	SunDu-derived	2.3*	-10.6**	1.2	-1.9**
	SunDu-derived_HM	1.6	-1.2	1.4	0.9*
Radiative Effect	CCRE series	-1.1	-1.4	-0.0	-1.4**
	Residual series	2.4**	-0.1	1.2*	2.2**

740

741

742

743 <sup>a</sup>The trend calculations were based on the linear regression method. Values with two  
 744 asterisks (\*\*) imply  $p < 0.01$ , and those with one asterisk (\*) imply  $0.01 < p < 0.1$ .

745 <sup>b</sup> $R_s$  trends were calculated by different numbers of observations, including all stations  
 746 that are available on the JMA website and 41 stations (marked with red in Table S1,  
 747 detailed in Section 3.1) that are significantly improved after homogenization. This  
 748 implies that the sample number has a subtle impact on the trend calculation over Japan.

749 Radiative effects from clouds and aerosols were also explored.

750 <sup>c</sup>Trend calculations were based on the raw measurements of surface incident solar  
 751 radiation (OBS-raw), their homogenized series (OBS\_HM), derived incident solar  
 752 radiation from sunshine duration hours (SunDu-derived) and their homogenized series  
 753 (SunDu-derived\_HM). OBS\_HM from 1961 to 1970 was further homogenized by  
 754 using SunDu-derived\_HM as reference data, termed OBS\_2HM. It is found that

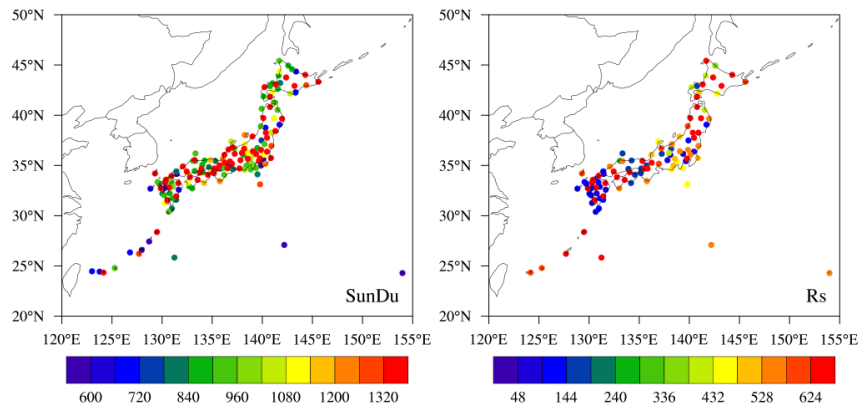
755 homogenized SunDu-derived  $R_s$  have the lowest uncertainties among these five  
756 datasets in Section 3.1. The cloud cover radiative effect (CCRE) was denoted as the  
757 change in  $R_s$  produced by a change in cloud cover, and the CCRE calculations were  
758 performed following Equation (4) by observed cloud amounts and the cloud radiative  
759 effect (CRE) from CERES satellite retrieval. Residual effect series were obtained by  
760 removing the CCRE from homogenized SunDu-derived  $R_s$  anomalies.  
761

762

763 Table 2. Trends of Surface Incident Solar Radiation ( $R_s$ ) in Japan during Specific Time764 Periods for Different Types of Datasets for All Seasons. Unit:  $W\ m^{-2}$  per decade

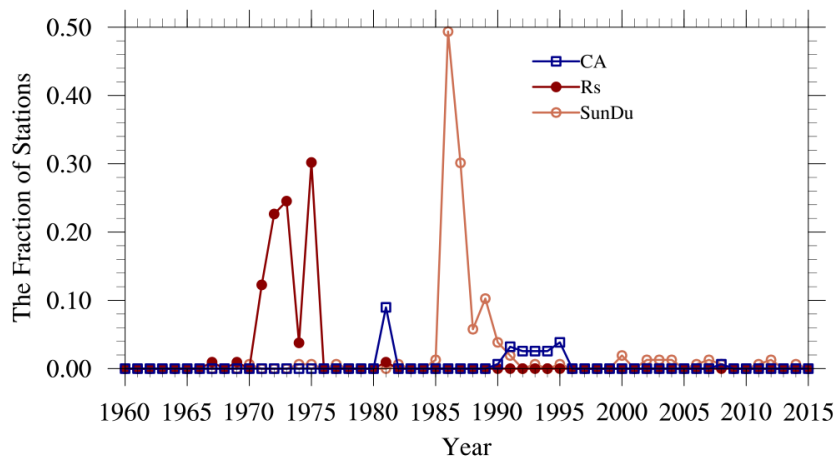
Season	Datasets	1961-1980	1981-1995	1996-2014	1961-2014
Spring	SunDu-derived_HM	3.1	-1.5	3.4*	1.5
	CCRE series	-0.7	-1.6	-1.6	-0.9
	Residual series	4.9**	-0.5**	2.2**	2.8*
Summer	SunDu-derived_HM	1.4	-3.4	0.6	0.4
	CCRE series	-1.9	-2.1	-4.4**	-2.7
	Residual series	2.0**	-1.8	1.5**	2.8
Autumn	SunDu-derived_HM	0.6	1.5	3.3**	1.0*
	CCRE series	-1.3**	1.6	1.6	-0.9
	Residual series	1.8**	0.8**	2.1**	2.0*
Winter	SunDu-derived_HM	0.6	-1.5	-1.6	0.5
	CCRE series	-0.6	-3.3	-0.6	-0.7
	Residual series	1.1**	0.9**	-0.9**	1.2**

765



766

767 Figure 1. The spatial distribution of stations over Japan with observed sunshine duration  
 768 (SunDu, 156 stations) and surface incident solar radiation ( $R_s$ , 105 stations) data. The  
 769 colours indicate the data length of the SunDu records from 1890 to 2015 and  $R_s$  records  
 770 from 1961 to 2015. Unit: month.

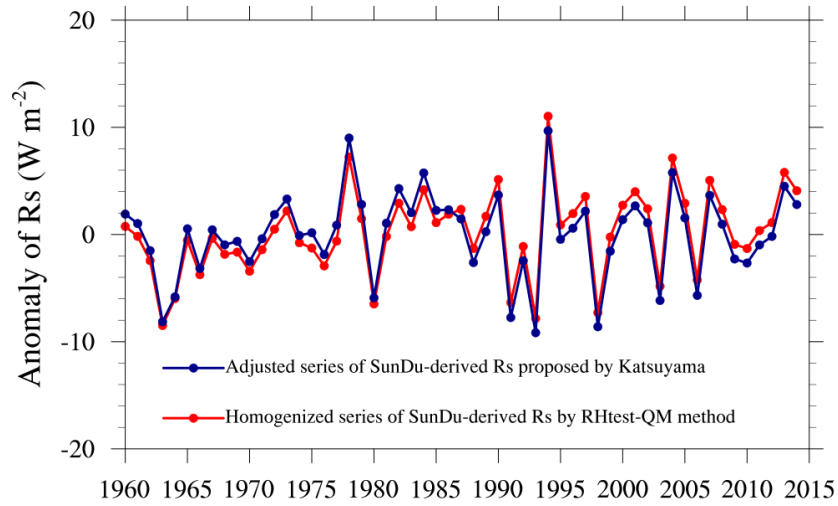


771

772 Figure 2. The fraction of stations that suffer from data inhomogeneity due to site  
 773 relocation, change of instruments and measurement method for sunshine duration  
 774 (SunDu) records, cloud amount (CA) records and surface incident solar radiation ( $R_s$ )  
 775 records. In total, there were 156 stations with SunDu records, 105 of which had  $R_s$   
 776 records and 155 of which had CA records. The inhomogeneity information shown here  
 777 was derived from metadata from  
 778 <https://www.data.jma.go.jp/obd/stats/data/en/smp/index.html>, and was used as primary  
 779 information to perform the inhomogeneity adjustment in the RHtest method detailed in  
 780 Section 2.2.

781

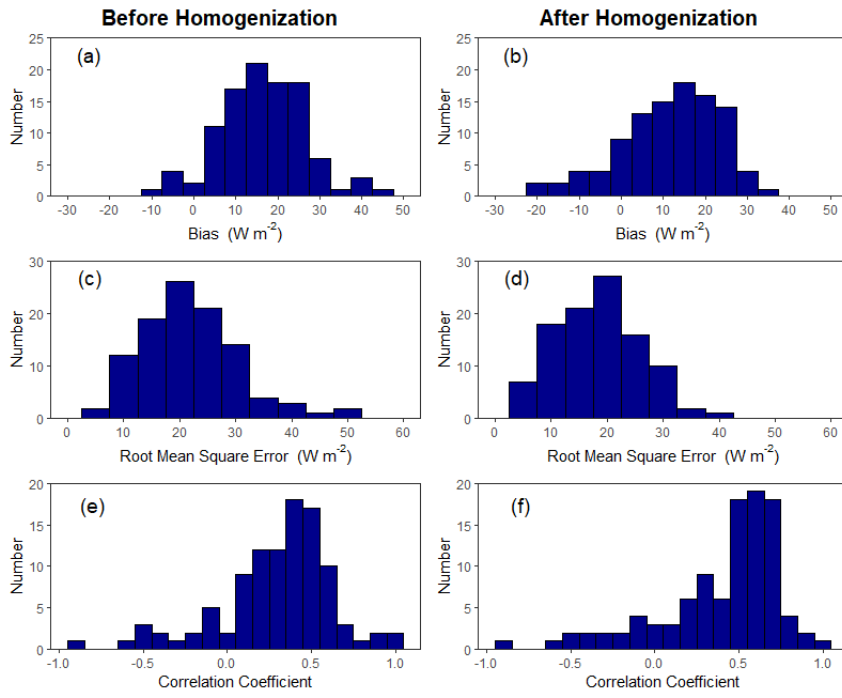
782



783

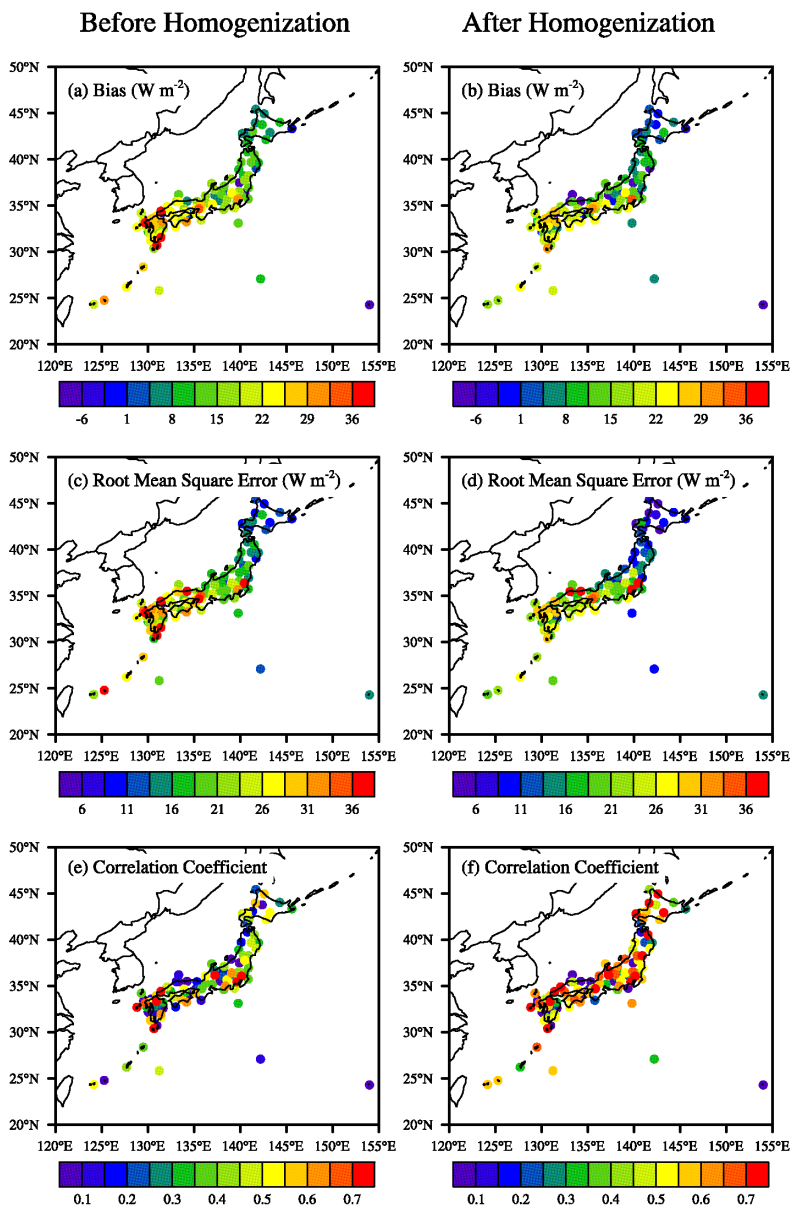
784 Figure 3. The anomalies of surface incident solar radiation ( $R_s$ ) derived from  
 785 homogenized sunshine duration (SunDu) data (red line) by the RHtest-QM method  
 786 and other independent data (blue line) adjusted by the method in (Katsuyama, 1987).  
 787 Both of the homogenized datasets yield nearly the same  $R_s$  variation.

域代码已更改



带格式的：居中





790

791 Figure 4. The spatial distribution of Histograms of bias, root mean square error and

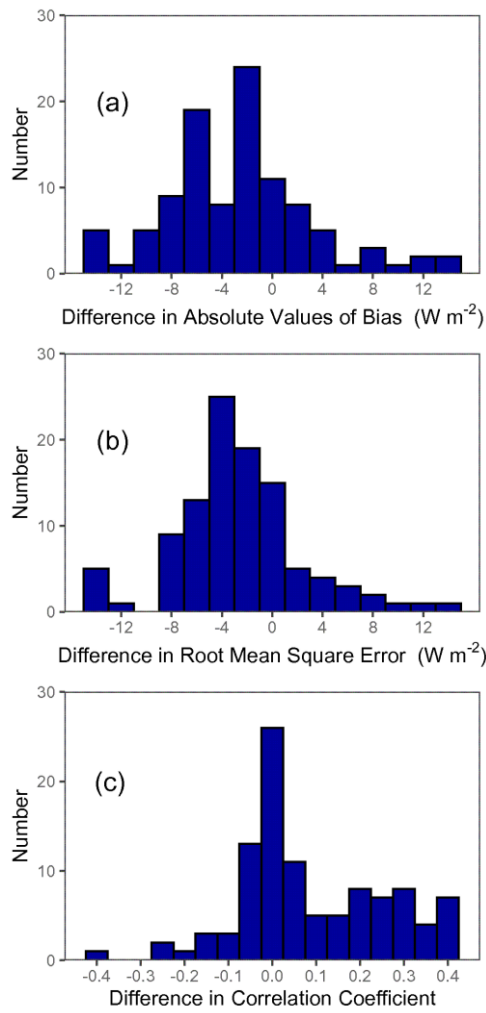
792 correlation coefficient between SunDu-derived surface incident solar radiation ( $R_s$ )

793 and observed  $R_s$  before (a, c, e) and after (b, d, f) homogenization. Improvements

794 were ~~Their differences decrease~~ made at most sites after homogenization.

795 \_\_\_\_\_

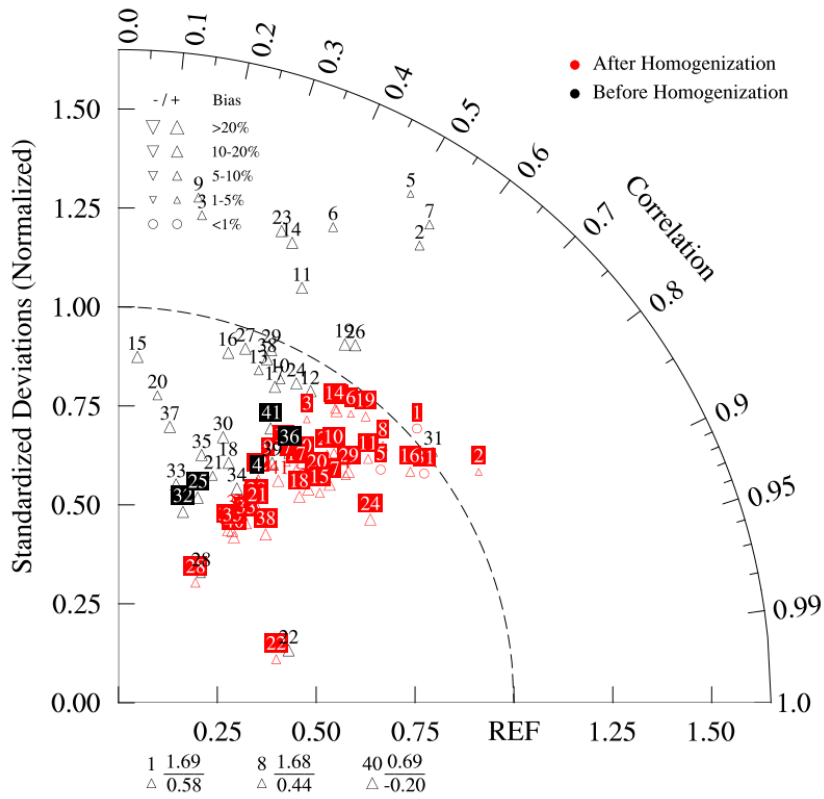
796



797

798 Figure 5. Histograms of the difference in absolute values of bias, root mean square  
799 error and correlation coefficient between SunDu-derived surface incident solar  
800 radiation ( $R_s$ ) and observed  $R_s$  before and after homogenization. Their differences  
801 decrease after homogenization.

802  
803  
804



805

806

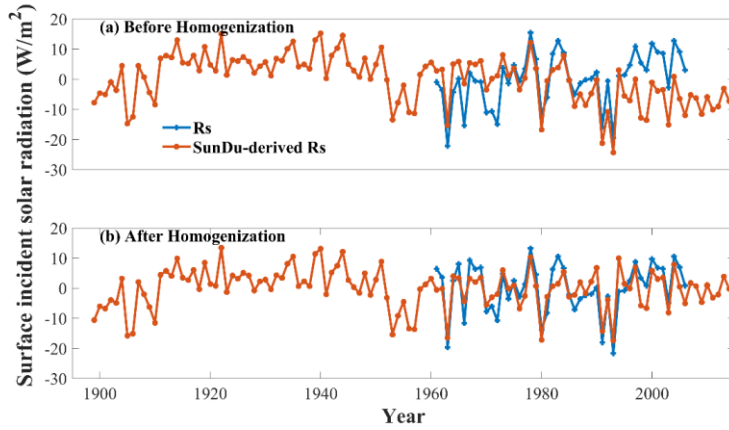
807 Figure 6. Taylor diagram describing the relative biases, standardized deviations and  
808 correlation coefficients between the annual observed surface incident shortwave  
809 radiation (Rs) and annual sunshine duration (SunDu) derived Rs before and after  
810 homogenization at 41 selected stations (Numbered 1-41 here). “REF” can be treated as  
811 the perfect point, where values the closer to this point indicate a better evaluation. The

812 size and direction of the triangles denote the magnitude and negative or positive of  
813 biases, respectively. The boxes indicate the smaller bias in Raw (black color) or HM  
814 (red color) series. This figure shows that biases decrease at most sites (in red boxes)  
815 after homogenization, except for the 5 stations numbered 4, 25, 32, 36 and 41 (in black  
816 boxes). Three stations (numbered 1, 8 and 40 in black color) listed below the panel are  
817 beyond the scope of the figure, with bias (triangle), ratio of standardized deviation  
818 (above the “---” line) and correlation coefficient (below the “---” line) shown. In  
819 addition to the improvements in the correlation coefficients after homogenization, the  
820 biases and the standard deviations generally become small in this Taylor diagram.

821

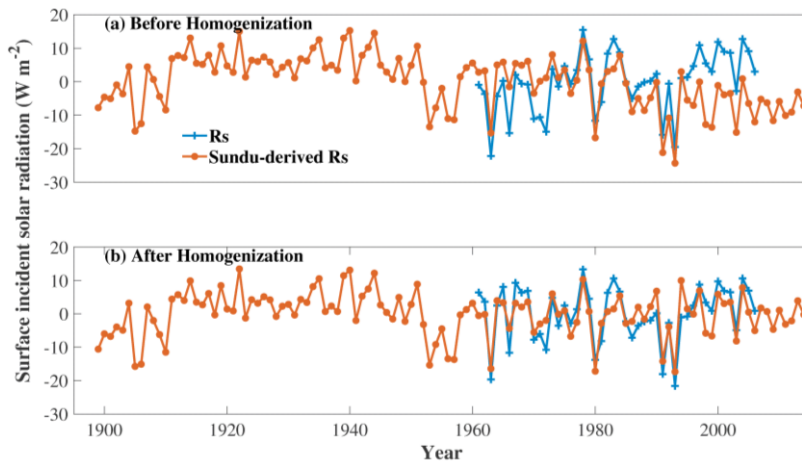
822 \_\_\_\_\_

823



824

825



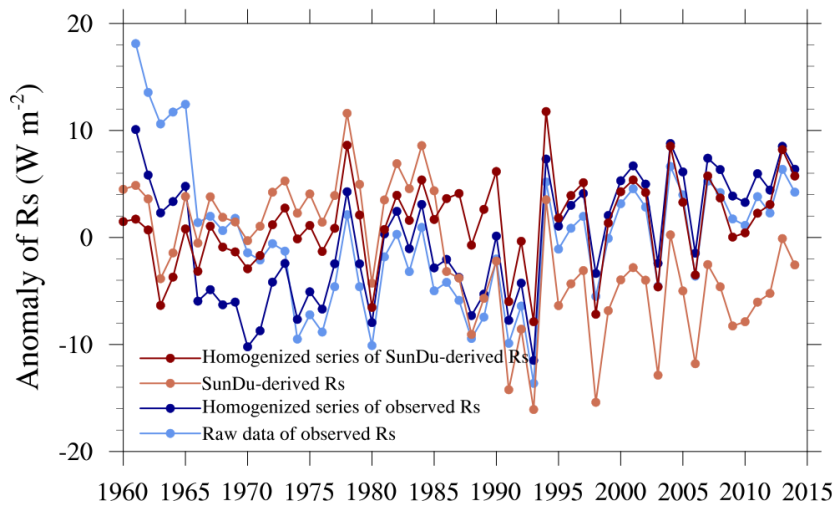
826

827

828 Figure 57. Time series of annual anomalies of observed surface incident solar radiation  
829 ( $R_s$ ) and SunDu-derived  $R_s$  at HAMADA site (WMO-ID: 47755, Lat: 34.9° , Lon:  
830 132.07) before and after homogenization.

831

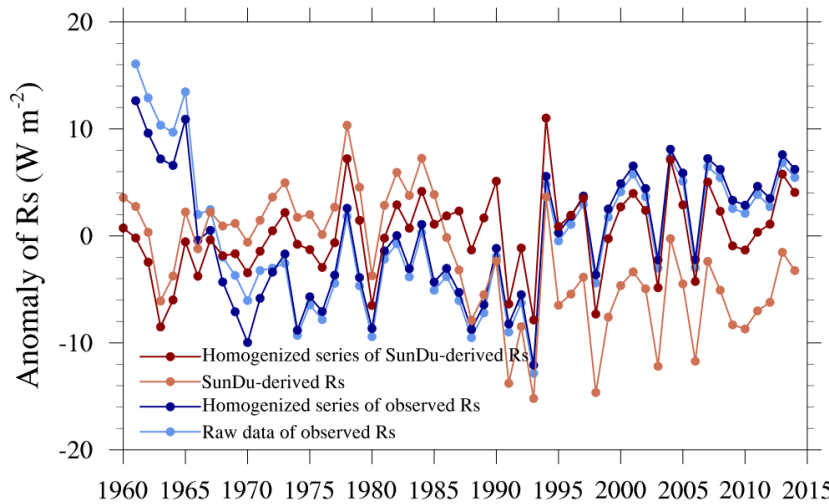
832



833

834 Figure 68. Time series of annual anomalies of surface incident solar radiation ( $R_s$ ) based  
 835 on direct  $R_s$  observations (light blue line) and their homogenized series (dark blue line)  
 836 and sunshine duration (SunDu) derived  $R_s$  (light red line) and their homogenized series  
 837 (dark red line). All of the lines were calculated based on observations at 41 sites. Details  
 838 on how these 41 sites were selected are given in Section 3.1. The  $R_s$  variations are nearly  
 839 the same as those shown in Figure 7, which were calculated based on all available  
 840 observations.

841



842 1960 1965 1970 1975 1980 1985 1990 1995 2000 2005 2010 2015

843 Figure 79. Time series of annual anomalies of the surface incident solar radiation ( $R_s$ )

844 based on direct observations (light blue line) and their homogenized series (dark blue

845 line) and sunshine duration (SunDu) derived  $R_s$  (light red line) and their homogenized

846 series (dark red line). All of the lines were calculated based on as many observations as

847 possible. The light blue line and dark blue line were calculated from the  $R_s$  observations

848 at 105 sites, while the light red line and dark red line were derived from the SunDu-

849 derived  $R_s$  at 156 sites. The  $R_s$  variations are nearly the same as those shown in Figure

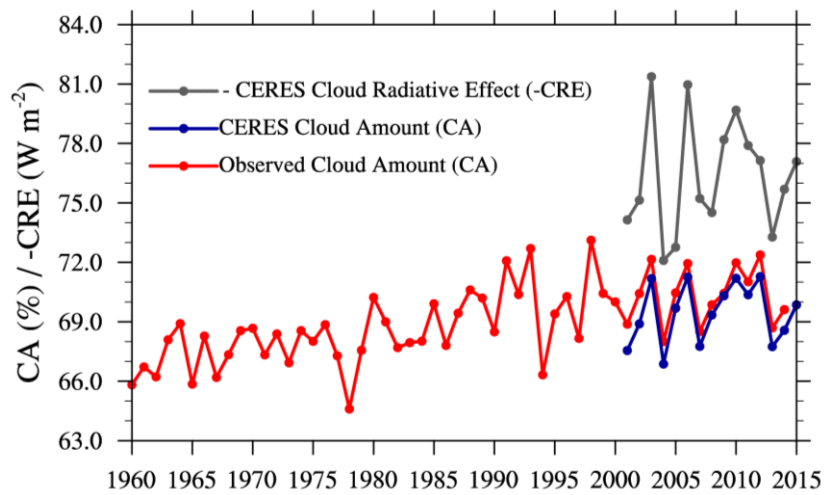
850 6, which were calculated based on the 41 selected sites in Section 3.1. Large

851 discrepancies were found in the homogenized data series (dark blue and dark red lines).

852

853





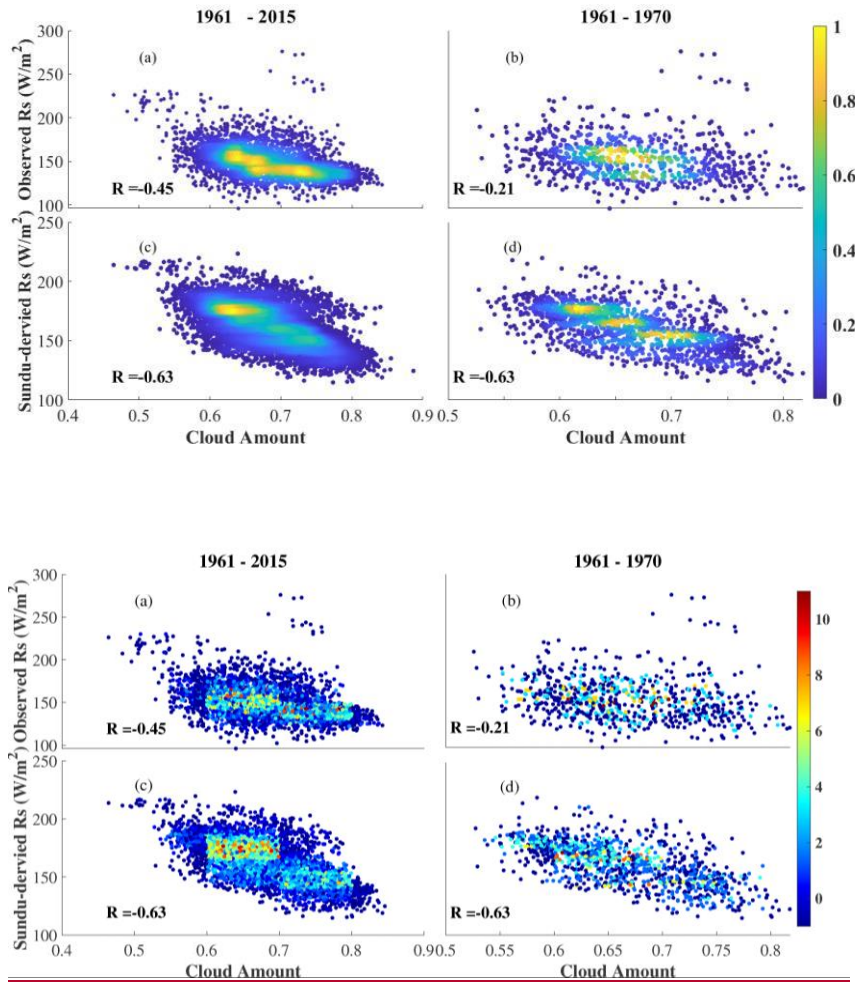
854

855 Figure 8.10. The cloud amount (CA) from CERES (blue line) agrees well with that  
 856 derived from surface observations (red line) over Japan. At the annual time scale, the  
 857 negative cloud radiative effect (-CRE, grey line) in CERES correlated well with the  
 858 cloud amount.

859

860

861



862

863

864

865 Figure 911. Scatter plot of homogenized monthly surface incident solar radiation ( $R_s$ )

866 (observed and SunDu-derived solar radiation) as a function of ground-based

867 observations of cloud amount over Japan at all stations only when both cloud amount

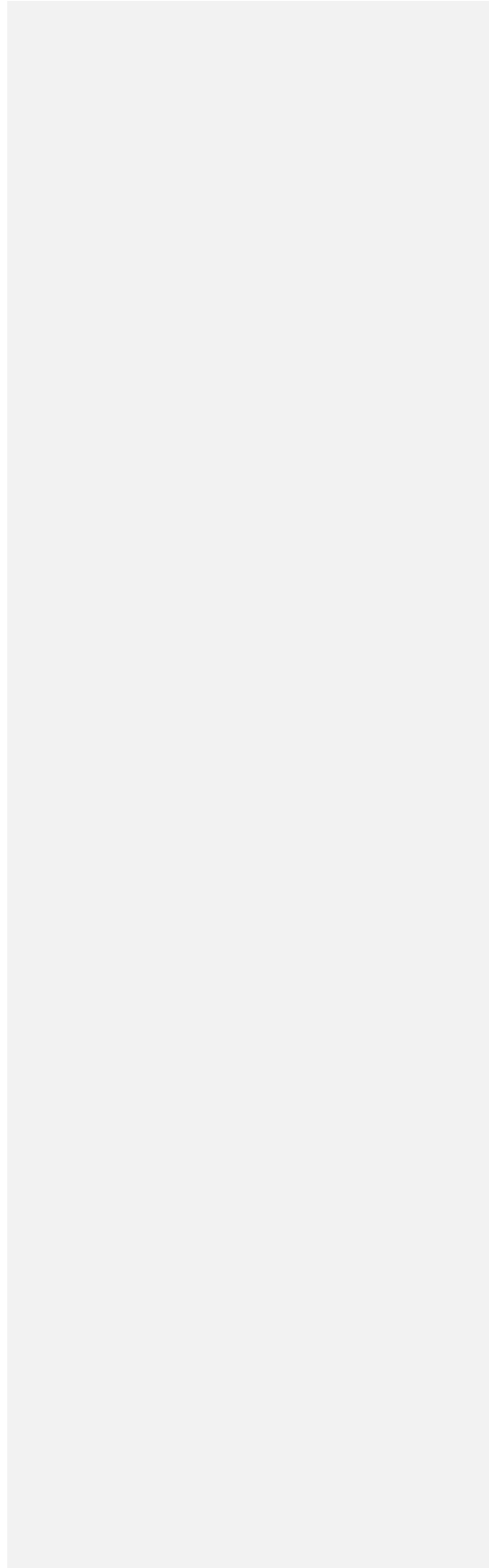
868 data and observed  $R_s$  data are available. (a) and (c) for 1961-2015, (b) and (d) for

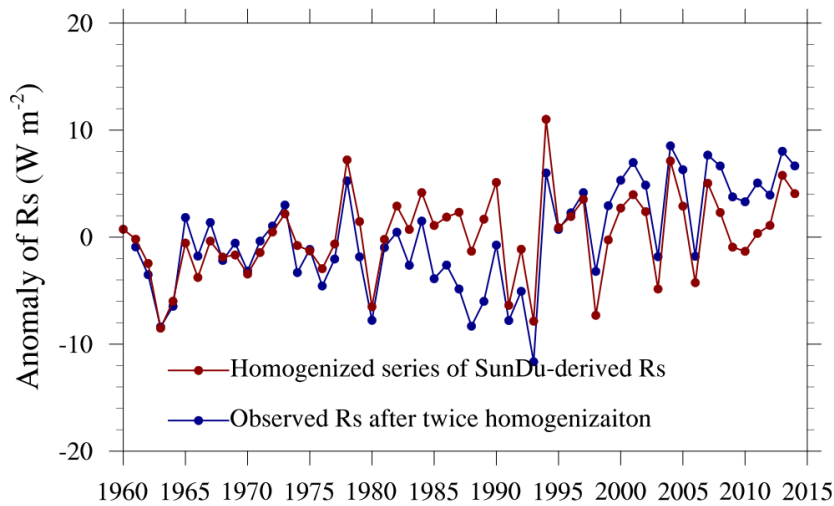
869 1961-1970. The smallest correlation coefficient in (b) indicates that the observed  $R_s$

870 data are spurious for 1961-1970, and SunDu-derived  $R_s$  are more convincing.

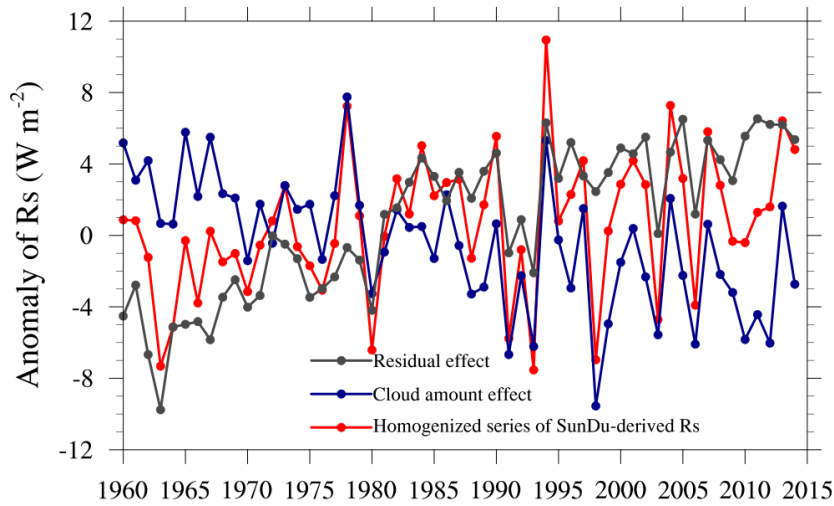
871

51





872  
 873 Figure 4012. Time series of annual anomalies of the surface incident solar radiation ( $R_s$ )  
 874 based on  $R_s$  observations after two homogenizations (dark blue line). The homogenized  
 875 series of observed  $R_s$  from 1961 to 1970 shown in Figure 7 was tuned by RHtest method  
 876 again using the homogenized series of SunDu-derived  $R_s$  (dark red line in Figure 7 and  
 877 Figure 10) as a reference.



878

879 Figure 44.13. Area-averaged anomalies of homogenized SunDu-derived  $R_s$  (red line)

880 over Japan. The cloud cover radiative effect (CCRE, blue line) was denoted as the

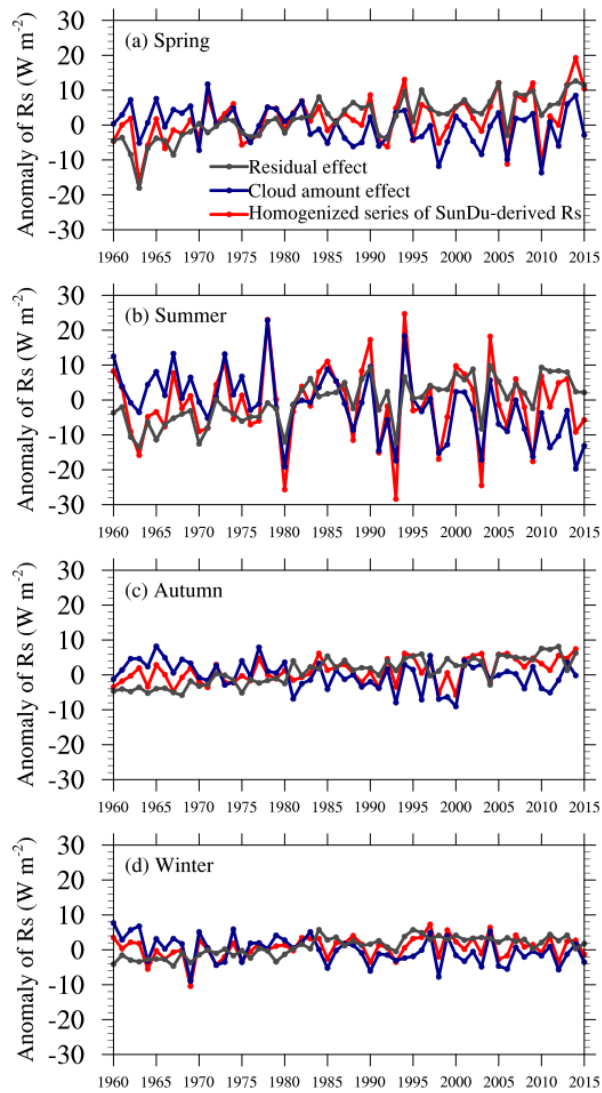
881 change in  $R_s$  produced by a change in cloud cover and calculated following Equation

882 (4) by observed cloud amounts and cloud radiative effect (CRE) from the CERES

883 satellite retrieval. The residual effect (grey line) was obtained by removing the cloud

884 cover radiative effect (CCRE) from the homogenized SunDu-derived  $R_s$  anomalies.

885



886

887 Figure 12-14. Same as Figure 10-12 but for the four seasons. The decrease in Asian  
 888 spring dust may have triggered the brightening over Japan for 1961-2015, as the  $R_s$  in  
 889 spring increases most among the seasons.

带格式的: 字体颜色: 自动设置

带格式的: 字体颜色: 自动设置